Drosophila APC2 Is a Cytoskeletally-associated Protein that Regulates Wingless Signaling in the Embryonic Epidermis

Brooke M. McCartney,* Herman A. Dierick,‡ Catherine Kirkpatrick,* Melissa M. Moline,‡ Annette Baas,* Mark Peifer,* and Amy Bejsovec‡

*Department of Biology, University of North Carolina at Chapel Hill, Chapel Hill, North Carolina 27599-3280; and
‡Department of Biochemistry, Molecular Biology, and Cell Biology, Northwestern University, Evanston, Illinois 60208-3500

Abstract. The tumor suppressor adenomatous polyposis coli (APC) negatively regulates Wingless (Wg)/Wnt signal transduction by helping target the Wnt effector β-catenin or its *Drosophila* homologue Armadillo (Arm) for destruction. In cultured mammalian cells, APC localizes to the cell cortex near the ends of microtubules. *Drosophila* APC (dAPC) negatively regulates Arm signaling, but only in a limited set of tissues. We describe a second fly APC, dAPC2, which binds Arm and is expressed in a broad spectrum of tissues. dAPC2's subcellular localization revealed colocalization with actin in many but not all cellular contexts, and also suggested a possible interaction with astral microtubules. For example, dAPC2 has a striking asymmetric distribution in neuroblasts, and dAPC2 colocalizes with assembling actin filaments at the base of developing larval denticles. We identified a *dAPC2* mutation, revealing that dAPC2 is a negative regulator of Wg signaling in the embryonic epidermis. This allele acts genetically downstream of *wg*, and upstream of *arm*, *dTCF*, and, surprisingly, *dishevelled*. We discuss the implications of our results for Wg signaling, and suggest a role for dAPC2 as a mediator of Wg effects on the cytoskeleton. We also speculate on more general roles that APCs may play in cytoskeletal dynamics.

Key words: *Drosophila* • adenomatous polyposis coli • Armadillo • β-catenin • Wingless

HUMAN β-catenin (βcat)[1] and its *Drosophila* homologue Armadillo (Arm) are key effectors of the conserved Wingless (Wg)/Wnt signal transduction pathway (for review see Gumbiner, 1998). In the absence of Wg signal, Arm in the cytoplasm is targeted for destruction by a multiprotein complex. Wg signal inactivates the destruction machinery, permitting accumulation of Arm in the cytoplasm and nucleus. Arm forms a complex with the DNA-binding protein, dTCF, to alter expression of Wg-responsive genes. Wnt signaling was implicated in colon cancer through the study of familial adenomatous polyposis, an inherited disease which results in early-onset colon cancer due to an increase in the frequency of benign colon polyps. These patients are heterozygous for a mutation in the adenomatous polyposis coli (APC) tumor suppressor; somatic disruption of the second copy of *APC* initiates polyp development (for review see Polakis, 1999). APC is part of the Arm/βcat destruction complex, along with Axin and the kinase Zeste-white 3 (Zw3)/glycogen synthase kinase 3β (GSK). In cells of a colon polyp, loss of APC function disables the destruction complex, leading to βcat accumulation, formation of βcat–TCF complexes, and activation of Wnt target genes such as the oncogene c-myc. APC is also important during normal development: mice homozygous for *APC* mutations die before gastrulation (Moser et al., 1995). A *Drosophila* homologue of APC, *dAPC* (Hayashi et al., 1997), acts as a negative regulator of Arm signaling in the photoreceptors of the developing adult eye (Ahmed et al., 1998).

APC's biochemical function in the destruction complex remains somewhat mysterious. It is thought to be a protein scaffold that binds numerous protein partners at distinct sites along its length (see Fig. 1) (for review see Polakis, 1999). APC was thought to facilitate interaction between βcat and GSK. However, Axin can also link βcat, GSK, and APC, raising questions about APC's role. Work in the nematode *Caenorhabditis elegans* suggests that APC's role

H.A. Dierick and C. Kirkpatrick contributed equally to this paper.

Address correspondence to Mark Peifer, Department of Biology, Coker Hall, CB#3280, University of North Carolina at Chapel Hill, Chapel Hill, NC 27599-3280. Tel.: (919) 962-2271. Fax: (919) 962-1625. E-mail: peifer@unc.edu; or Amy Bejsovec, Department of Biochemistry, Molecular Biology, and Cell Biology, Northwestern University, 2153 Sheridan Rd., Evanston, Illinois 60208-3500. Tel.: (847) 467-4042. Fax: (847) 467-1380. E-mail: bejsovec@nwu.edu

1. *Abbreviations used in this paper:* AEL, after egg laying; APC, adenomatous polyposis coli; Arm, Armadillo; βcat, β-catenin; BicD, Bicaudal D; Dsh, Dishevelled; dAPC, *Drosophila* APC; Fz, Frizzled; GSK, glycogen synthase kinase 3β; hAPC, human APC; Insc, Inscuteable; IP, immunoprecipitate; MT, microtubule; PP2A, protein phosphatase 2A; Wg, Wingless; Zw3, Zeste-white 3.

in Wnt signaling is more complex. Disruption of the closest nematode APC relative, *apr-1* (by double-stranded RNA interference), unexpectedly led to a phenotype similar to that of loss-of-function mutations in Wnt and Arm relatives, suggesting that APR-1 is a positive effector of Wnt signaling (for review see Han, 1997).

APC may also have additional cellular roles. When human APC (hAPC) is overexpressed in cultured cells, it decorates microtubules (MTs) and can bind and bundle MTs in vitro (Munemitsu et al., 1994; Smith et al., 1994). In cultured cells, APC localizes at the cell cortex in membrane puncta where bundles of MTs often terminate (Näthke et al., 1996). If one expresses a stabilized form of βcat (which cannot be phosphorylated by GSK) in MDCK cells, mutant βcat accumulates with APC in membrane puncta, and these cells display altered migratory behavior (for review see Barth et al., 1997). These data prompted the suggestion that APC may regulate cell migration via its interaction with MTs, and that this role is modulated by βcat. APC may also influence cytoskeletal dynamics by binding to EB1 (Su et al., 1995), which associates with the MT cytoskeleton in mammalian cells (Berrueta et al., 1998; Morrison et al., 1998). Yeast EB1 homologues contribute to MT function and may form part of a cytokinesis checkpoint (Beinhauer et al., 1997; Schwartz et al., 1997; Muhua et al., 1998). In addition to connections with MTs, APC may associate with the actin cytoskeleton via β- and α-catenin.

The actin and MT cytoskeletons are both targets of the Wg/Wnt pathway. Signaling by Wnt family members or by their Frizzled (Fz) receptors is required to orient certain cell divisions in both nematodes and flies. In *C. elegans*, Wnt signaling directs the orientation of mitotic spindles in specific early embryonic blastomeres and orients postembryonic asymmetric cell divisions (for review see Han, 1997), whereas in *Drosophila* Fz is required for orientation of the mitotic spindles of bristle precursor cells (Gho and Schweisguth, 1998). Fz also plays a key role in orienting the cytoskeleton during formation of hairs and bristles, polarized outgrowths of the cell membrane (for review see Shulman et al., 1998). Both the actin and MT cytoskeletons are required for hair positioning and growth (Wong and Adler, 1993; Turner and Adler, 1998).

Whereas dAPC regulates Arm signaling in the *Drosophila* larval photoreceptors (Ahmed et al., 1998), two features of dAPC were surprising given the widespread expression and essential function of mouse APC. Embryonic expression of dAPC is largely confined to the central nervous system (Hayashi et al., 1997), and null mutations in *dAPC* are viable and fertile, with strong effects only in the larval photoreceptors (Ahmed et al., 1998). These observations suggested the existence of a second APC gene in flies; a second mammalian APC has been identified (Nakagawa et al., 1998; van Es et al., 1999).

Materials and Methods

Biochemistry and Two-Hybrid Analysis

Extract preparation, immunoprecipitations (IPs), cell fractionation, and analysis of phosphorylation were as in Peifer (1993); anti-Arm IPs were at 1:40 and anti-dAPC2 IPs at 1:50. Samples were analyzed by 6% acrylamide SDS-PAGE, transferred to nitrocellulose, and immunoblotted with rat anti-dAPC2 (1:500), or mouse mAbs anti-Arm(7A1) at 1:500 (Peifer, 1993), anti–Bicaudal D (BicD) at 1:50, and anti–β-tubulin (Amersham Pharmacia Biotech) at 1:100, followed by ECL (Amersham Pharmacia Biotech) detection. Two-hybrid experiments were as in Pai et al. (1996). Yeast cells were transformed with plasmids encoding portions of the Arm repeat region fused to the LexA DNA binding domain and encoding fragments of dAPC or dAPC2 fused to the GAL4 activation domain; the control plasmid pCK4 expresses only the activation domain. Values are averages of duplicate β-galactosidase assays on more than six independent transformants.

Immunolocalization

Anti-dAPC2 antisera were raised in rats by Pocono Rabbit Farms against a GST-dAPC2 (amino acids 491–1061) fusion. Embryos were fixed in 37% formaldehyde/heptane (1:1) for 5 min (for anti–β-tubulin antibody, fix was 50 mM EGTA, pH 8, 33% formaldehyde). Larval tissues were fixed in 4% paraformaldehyde in PBS for 20 min. All were blocked and stained in PBS with 1% goat serum and 0.1% Triton X-100. Antibodies were used as follows: anti-dAPC2, 1:1,000; rabbit polyclonal antibody anti-Arm, 1:100; anti–β-tubulin (Amersham Pharmacia Biotech) 1:100; rhodamine phalloidin (Molecular Probes), 1:1,000; antiphosphohistone (Upstate Biotechnology), 1:200; anti-Prospero, 1:5 (kindly provided by C. Doe, University of Oregon, Eugene, OR).

Genetic Analysis

dAPC2$^{\Delta S}$ was induced by ethyl methanesulfonate (EMS) in a screen for suppressors of *wg*^{PE4}. *dAPC2*$^{\Delta S}$ also suppresses the null allele *wg*^{CX4}. Further analysis revealed that *dAPC2*$^{\Delta S}$ is a homozygous viable, temperature-sensitive maternal-effect lethal mutation mapping to 95E–F. Stocks for epistasis analysis were constructed at 18°C. Epistasis analysis was conducted at 25°C as in Table I. Antibody staining and RNA in situ hybridization were as in Dierick and Bejsovec (1998). Cuticle preparations were as in Wieschaus and Nüsslein-Volhard (1986). Genomic DNA from *dAPC2*$^{\Delta S}$ homozygotes, from the background chromosome, and from two wild-type stocks was subjected to PCR with overlapping sets of primers. PCR products were analyzed both by direct sequencing and by cloning into TA-vectors (Promega) and sequencing at least two independent clones.

Results

A Second Drosophila APC

10 expressed sequence tags from the Berkeley *Drosophila* Genome Project correspond to *dAPC2*; we obtained sequence of several cDNAs and the corresponding genomic region (we reported partial sequence in van Es et al., 1999; full sequence data available from EMBL/GenBank/DDBJ under accession no. AF091430). These predict a 1067 amino acid protein with striking similarity to other APC family members (Fig. 1) (for review of hAPC features see Polakis, 1999). All share an NH_2-terminal conserved domain, 6 Arm repeats, and a series of βcat binding (15 and 20 amino acid repeats) and Axin binding (SAMP repeats; Behrens et al., 1998) motifs. dAPC2 is shorter at its NH_2 and COOH termini than other APCs. dAPC2 lacks the COOH-terminal basic region (the putative MT binding site) found in hAPC and dAPC (Hayashi et al., 1997), as well as the hAPC region containing binding sites for Discs-large (DLG) and EB1. Substantial alternative splicing is unlikely, as there are only two small introns in coding sequences (63 and 197 nucleotides).

dAPC2 is most similar to other APC family members in the Arm repeats, where it most closely resembles dAPC; hAPC2 is more similar to hAPC (Fig. 1 B) (dAPC2 is 81% identical to dAPC and 57% identical to hAPC). Thus,

Table I. Drosophila Melanogaster Stocks Used in Epistasis Tests

Gene	Cross scheme	Results
wg	*wg^{CX4}/CyO; dAPC2$^{\Delta S}$* females ×× males	All *wg* progeny show the suppressed phenotype ($n > 100$).
	wg^{CX4}/CyO; dAPC2$^{\Delta S}$/Df(3R)crb87-4 females ×× *wg^{CX4}/+; +/Df(3R)crb87-4* males	1/3 of *wg* progeny show the suppressed phenotype ($n = 40$, *Df* homozygotes show *crumbs* phenotype).
arm	*arm$^{H8.6}$/FM7/dAPC2$^{\Delta S}$* females ×× *dAPC2$^{\Delta S}$* males	1/4 of the progeny show the *arm* zygotic phenotype (presumably *arm$^{H8.6}$/Y; dAPC2$^{\Delta S}$* male embryos). 3/4 show excess naked cuticle like *dAPC2$^{\Delta S}$* single mutants ($n > 200$).
dTCF	*dAPC2$^{\Delta S}$; dTCF^{3}/ey^{D}* females ×× males	1/4 of the progeny show the *dTCF* zygotic phenotype, and the remainder have excess naked cuticle ($n > 200$).
dsh	1. *dsh^{75} FRT101/FM7; dAPC2$^{\Delta S}$*/TM6 females ×× *ovo^{D1} FRT101/Y; hsp-FLP(F38); dAPC2$^{\Delta S}$* males	Zygotic loss of *dsh* does not modify the *dAPC2$^{\Delta S}$* mutant phenotype.
	2. Heat-shock progeny as third instar larvae twice to induce recombination	
	3. From among progeny cross: *dsh^{75} FRT101/ovo^{D1} FRT101; dAPC2$^{\Delta S}$* females ×× 1. *dAPC2$^{\Delta S}$* males, 2. *dAPC2$^{\Delta S}$/Df(3R)crb87-4* males, or 3. *Df(3R)crb87-4/TM3* males	In the first ($n > 30$) and second ($n = 23$) crosses, 1/2 the progeny show the *dsh* germline clone mutant phenotype (presumed to be the *dsh^{75}/Y; dAPC2$^{\Delta S}$* male embryos) and 1/2 show a partially suppressed *dAPC2$^{\Delta S}$* mutant phenotype, due to paternal rescue of *dsh* ($n > 30$). The partial suppression of the *dAPC2$^{\Delta S}$* mutant phenotype is more dramatic ventrally, with most denticle belts fully formed; the dorsal surface is largely unrescued. In the cross to *Df(3R)crb87-4/TM3* males, some progeny hatch (presumably those that are paternally wild-type), but dead embryos show phenotypes identical to those in the other crosses ($n = 19$).

there is no correspondence between individual human and fly proteins, even though both phyla show neural-enriched isoforms, dAPC and hAPC2, suggesting independent gene duplications. All APCs have six Arm repeats; a putative seventh Arm repeat is much more divergent and is not identifiable in dAPC2. The NH_2-terminal conserved region (61% identity to dAPC vs. 44% identity to hAPC) distantly resembles the Arm repeat consensus and may form one or two degenerate Arm repeats. APC family members also share similarity COOH-terminal to the Arm repeats. hAPC has two sets of repeated βcat binding sites, the 15 and 20 amino acid repeats (for review see Polakis, 1999; dAPC features are from Hayashi et al., 1997; hAPC2 lacks 15 amino acid repeats). dAPC2 shares two of the three 15 amino acid repeats of dAPC. dAPC and dAPC2 have five 20 amino acid repeats, among which are interspersed SAMP repeats (Fig. 1 C). dAPC has four SAMP repeats, whereas dAPC2 has two. dAPC2 ends 40 amino acids after the last SAMP repeat.

dAPC2 Protein

We generated antisera to a dAPC2 fusion protein (amino acids 491–1061); antisera from two independent rats immunized with this antigen both recognize a single set of protein isoforms of ~155–170 kD in embryonic extracts (Fig. 2 A) (they occasionally weakly cross-react with proteins of ~120 and > 200 kD). In contrast, the preimmune sera do not recognize any proteins on immunoblots of embryo extract, supporting the specificity of the antisera. Further, as we show below, the migration on SDS-PAGE of the putative dAPC2 protein is altered in a *dAPC2* mutant, consistent with these protein isoforms representing the genuine dAPC2 protein. The predicted molecular mass of dAPC2, 117 kD, is smaller than the observed molecular mass. However, an epitope-tagged version of the dAPC2 open reading frame expressed in human SW480 colon carcinoma cells also migrated at much higher apparent molecular mass than predicted from the sum of the predicted molecular mass of the dAPC2 coding sequence plus that of the epitope (Fig. 2 A). This suggests that the large apparent molecular mass of dAPC2 is a property of its migration on SDS-PAGE. We examined the developmental profile of dAPC2 expression during embryogenesis (Fig. 2 B). dAPC2 is present in the preblastoderm embryo (presumably maternally contributed), and levels remain relatively constant through the first half of embryogenesis, then drop sharply.

As hAPC is phosphorylated (e.g., Rubinfeld et al., 1996), we suspected that the dAPC2 isoforms might be phosphorylation variants. To test this, we immunoprecipitated (IPed) dAPC2 from embryos and treated the IPs with protein phosphatase 2A (PP2A), a serine/threonine-specific phosphatase. PP2A treatment reduced the apparent molecular mass of dAPC2; this effect was abolished if the PP2A inhibitor okadaic acid was included during incubation (Fig. 2 C, left panel). Further, if embryonic cells were dissociated and incubated in tissue culture medium, the apparent molecular mass of dAPC2 decreased (Fig. 2 C, right panel); this effect was also abolished by okadaic acid, suggesting that it is mediated by endogenous phosphatases. Parallel alterations in Arm phosphorylation support this hypothesis (Fig. 2 C, right panel) (Peifer, 1993). Taken together, these data suggest that the dAPC2 isoforms reflect, at least in part, differential phosphorylation.

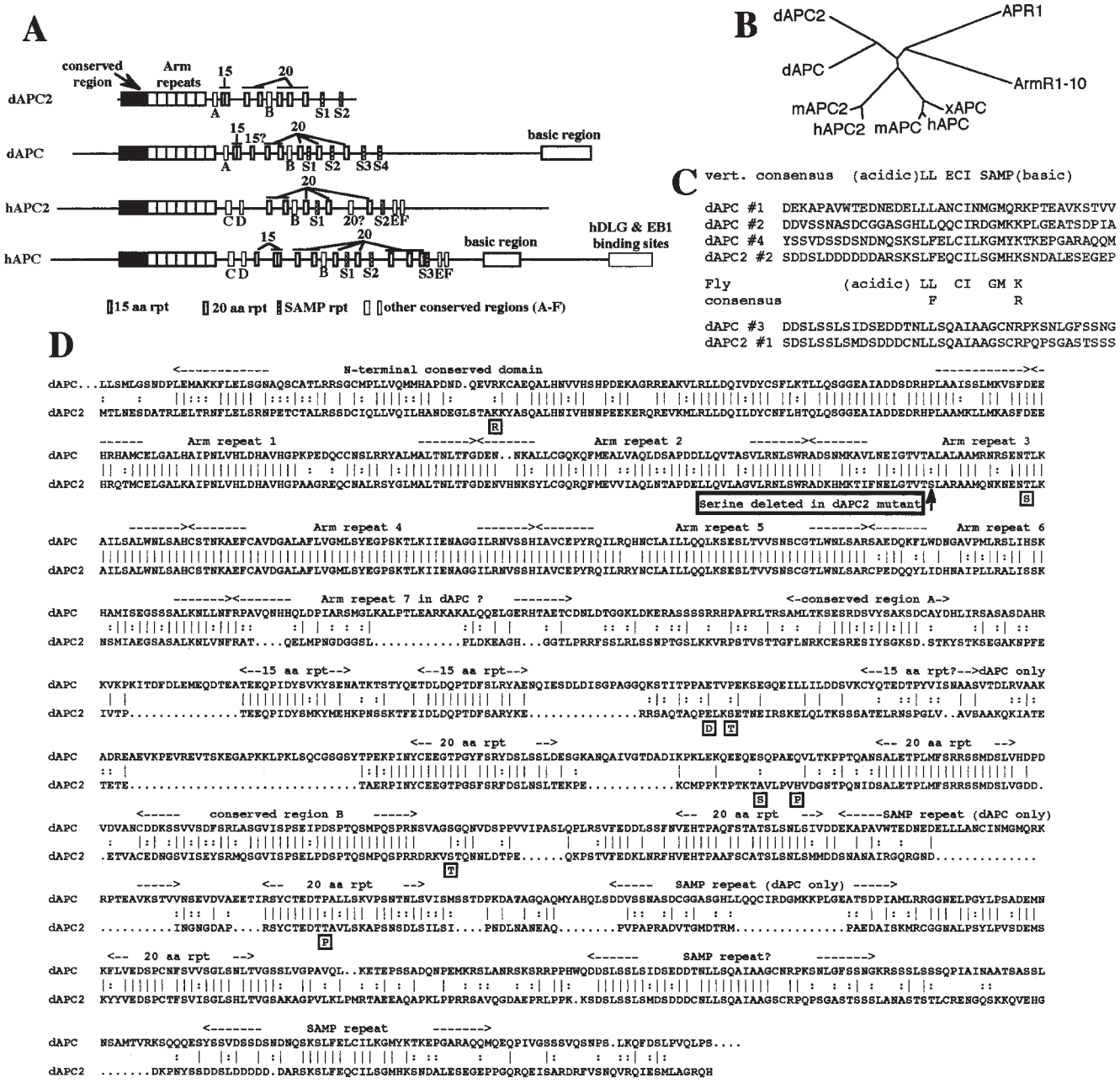

Figure 1. dAPC2. (A) Schematic diagrams of vertebrate and *Drosophila* APC proteins. Conserved sequence features are noted. A–F are conserved sequences of unknown function. The *dAPC2* start site was determined by the coincidence of the five longest Berkeley *Drosophila* Genome Project cDNAs and our 5′ rapid amplification of cDNA ends (RACE) cDNA products. (B) Unrooted tree showing relationships among the Arm repeats of APC family members from human, mouse, *Xenopus*, *Drosophila*, and *C. elegans*, as well as Arm repeats 1–10 of Arm. (C) Putative SAMP repeats of the *Drosophila* APCs. dAPC and dAPC2 share an additional sequence (bottom) which is a distant match to the SAMP motif. (D) Sequence comparison of dAPC and dAPC2, showing conserved domains. Below dAPC2 are listed polymorphisms on the background chromosome for $dAPC2^{\Delta S}$, and the position of the deleted serine in $dAPC2^{\Delta S}$. This residue is either serine or alanine in all APC family members, and this change is not found in five other wild-type strains.

dAPC2 Interacts Directly with Arm

hAPC and dAPC (Hayashi et al., 1997) bind to βcat and Arm, respectively. We tested whether dAPC2 also interacts with Arm in vivo. We immunoprecipitated Arm from embryonic extracts, and, in parallel, IPed proteins with a control mAb, anti-myc. dAPC2 specifically co-IPed with Arm from both early and older embryos (Fig. 2 D), but did not co-IP with the control anti-myc antibody. We were unable to detect Arm in anti-dAPC2 IPs (data not shown); because the antigen for the dAPC2 antisera includes the Arm binding region, these sera might not recognize a dAPC2–Arm complex. We also found that a dAPC2 fragment containing the putative βcat binding sites co-IPed with βcat when expressed in the human colorectal cancer cell line SW480 (data not shown).

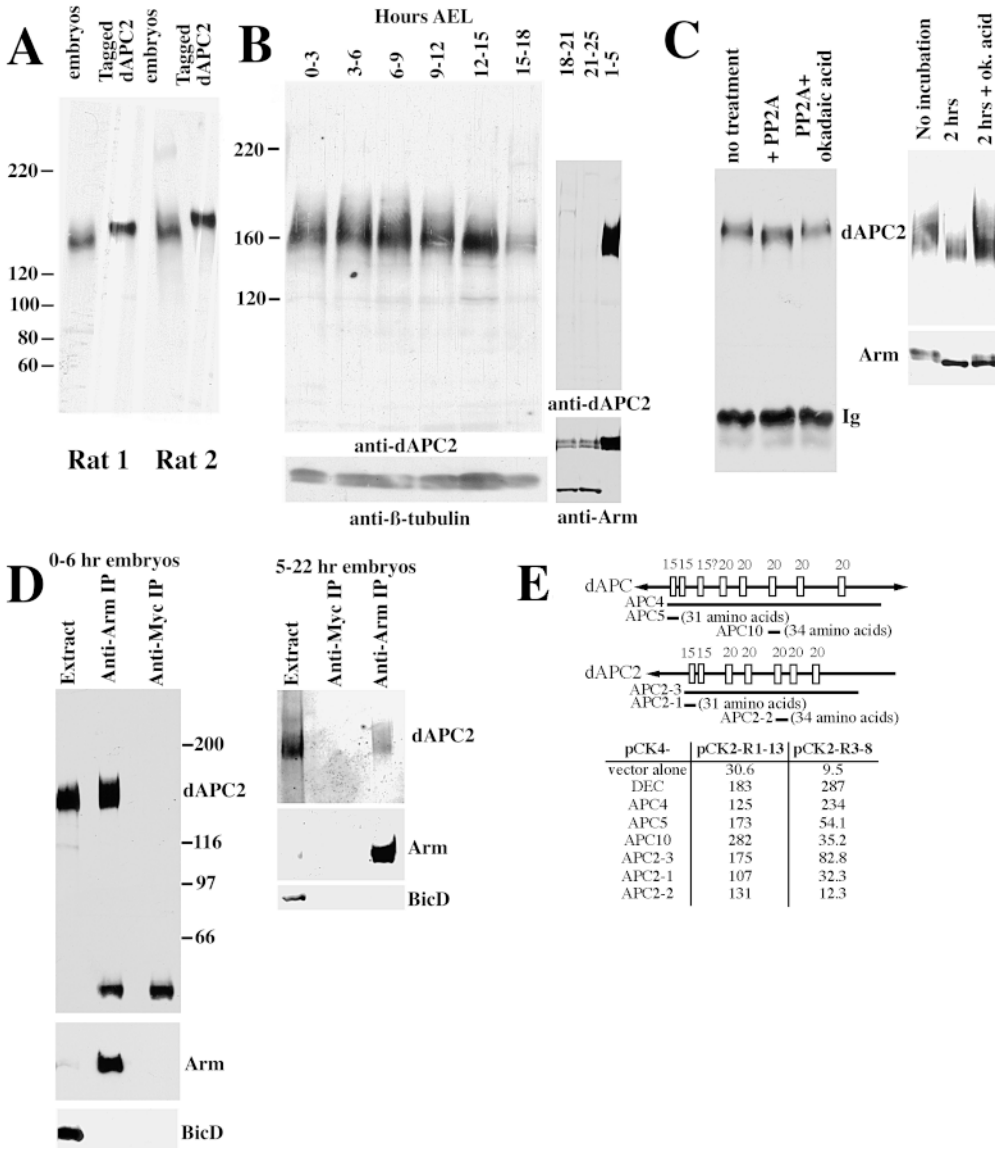

pCK4-	pCK2-R1-13	pCK2-R3-8
vector alone	30.6	9.5
DEC	183	287
APC4	125	234
APC5	173	54.1
APC10	282	35.2
APC2-3	175	82.8
APC2-1	107	32.3
APC2-2	131	12.3

Figure 2. dAPC2 protein properties. (A) dAPC2 protein. Extracts from 5–23-h *Drosophila* embryos and from human SW480 colon carcinoma cells expressing epitope-tagged dAPC2 coding sequences (the fusion protein includes a six-myc tag and additional amino acids at the fusion joint, raising its predicted molecular mass by 16 kD) were immunoblotted with anti-dAPC2 antisera from two independent rats immunized with our antigen. Most experiments in this paper were done with antisera from rat 2. (B) dAPC2 expression during embryogenesis. Extracts from embryos of the indicated ages AEL were immunoblotted with anti-dAPC2. β-Tubulin and Arm are loading controls. (C) dAPC2 is a phosphoprotein. (Left panel) Protein was immunoprecipitated from embryonic extracts with anti-dAPC2, left untreated, treated with PP2A, or treated with PP2A plus its inhibitor okadaic acid, and immunoblotted with anti-dAPC2. The apparent molecular mass of dAPC2 decreases upon phosphatase treatment. (Right panel) Dissociated gastrula stage embryonic cells were lysed immediately, or incubated in tissue culture medium for 2 h, in the absence or presence of the serine/threonine-specific phosphatase inhibitor okadaic acid. Extracts were immunoblotted with anti-dAPC2 or anti-Arm. During incubation, the apparent molecular mass of both dAPC2 and Arm is decreased; this is prevented by the phosphatase inhibitor. (D) dAPC2 associates with Arm in vivo. IPs with anti-Arm or anti-myc (a negative control) were done from embryonic extracts of 0–6-h (left panel) or 5–22-h (right panel) embryos. Extract and the IPs were immunoblotted with anti-dAPC2, anti-Arm, or anti-BicD (a negative control). dAPC2 specifically coimmunoprecipitated with anti-Arm. (E) dAPC2 binds Arm directly. β-Galactosidase activities were measured from yeast cells expressing the full Arm repeat region of Arm (pCK2-R1–13) or its centralmost Arm repeats (pCK2-R3–8) fused to a DNA-binding domain, together with various dAPC and dAPC2 fragments (diagrammed above) fused to a transcriptional activation domain. The empty vector and *Drosophila* E-cadherin (DEC) are negative and positive controls. Amino acid coordinates: APC4, APC5, and APC10 (751–1375, 751–781, and 1062–1095 of dAPC); APC2-3, APC2-1, and APC2-2 (491–991, 491–521, and 733–766 of dAPC2).

The hAPC–βcat interaction is direct, and is mediated by the 15 and 20 amino acid repeats of hAPC and the Arm repeats of βcat (for review see Polakis, 1999); the analogous region of dAPC binds Arm (Hayashi et al., 1997). To test whether dAPC2 directly interacts with Arm, we used the yeast two-hybrid system (Fig. 2 E), examining whether dAPC2's 15 and 20 amino acid repeats interact with the full set of Arm repeats of Arm (R1–13), or with the centralmost Arm repeats (R3–8; the binding site for *Drosophila* E-cadherin and dTCF). For comparison, we tested the 15 and 20 amino acid repeats of dAPC (Hayashi et al., 1997). The full 15 and 20 amino acid repeat regions of both dAPC and dAPC2 strongly interact with the entire Arm repeat region and with R3–8. We also tested 31–34 amino acid fragments carrying individual 15 or 20 amino acid repeats of dAPC and dAPC2 (selected as good matches to the consensus). Individual 15 amino acid repeats of either dAPC or dAPC2 interacted with both the entire Arm repeat region of Arm and with R3–8. An individual 20 amino acid repeat of dAPC also interacted with both Arm

fragments. A single 20 amino acid repeat of dAPC2 interacted strongly with Arm repeats 1–13; its interaction with R3–8 was much weaker.

dAPC2 Localization and the Actin and MT Cytoskeletons

To demonstrate that our anti-dAPC2 antisera are specific in situ, we determined that preimmune sera do not specifically stain any structures in *Drosophila* embryos, even at concentrations 10-fold higher than those we used below (data not shown). Our anti-dAPC2 sera also specifically stain mammalian cells engineered to express dAPC2 but not nontransfected cells (data not shown). The specificity of staining in situ is further supported by the change in intracellular localization seen in a dAPC2 mutant (see below), and by the fact that antisera from a second rat immunized with this antigen recognize a similar set of cellular structures (at least during midembryogenesis, the stage we examined).

Thus, we used our anti-dAPC2 antisera to characterize its expression and subcellular localization. During nuclear division cycles 10–13, which take place without cytokinesis in the peripheral cytoplasm of the embryo, dAPC2 shows dynamic changes in subcellular localization, coincident with those of actin (Fig. 3). Sequential changes in MT organization as nuclei proceed through mitosis direct reorganization of the cortical actin cytoskeleton (for review see Foe et al., 1993). Before nuclei migrate to the periphery, actin is found at the cortex in a random reticulum. When nuclei reach the periphery, actin condensations appear in interphase and prophase above each nucleus, forming an actin bud which overlays a cytoplasmic bud. This separates the mitotic apparatus of one nucleus from that of its neighbor. As division proceeds to metaphase, actin redistributes from the crown of the bud to its lateral cortex, forming an oblong ring around each spindle. During anaphase, actin redistributes into discs above each newly formed nucleus. Centrosomes and their associated MTs direct the changes in actin distribution, although the mechanism responsible for this interaction is not known.

In cycle 10–13 embryos, dAPC2 colocalizes with actin at all stages of mitosis (we could not test for colocalization with Arm, as its levels at these stages are too low to detect its localization). The dAPC2/actin colocalization is most prominent in the microvillar projections at the surface of the bud in interphase and prophase (Fig. 3, A–C). At metaphase and anaphase, dAPC2 and actin condensations are observed at the lateral cortex of the bud (Fig. 3, I–L); dAPC2 staining is somewhat less intense here relative to actin. Toward the base of the bud, condensations of actin and dAPC2 are also found in the region of the centrosome and asters (Fig. 3, E–H, arrows). These dAPC2 condensations occur within 0.3–0.5 μm of the surface of the embryo (data not shown), and thus are most prominent above the spindle apparatus; kinetochore MTs are not in uniform focus until ~1.25 μm from the surface of the embryo. The location of these dAPC2/actin condensations above the plane of the spindle places them in a position to interact with the astral MTs as they reach toward the cortex. During later nuclear cycles when pseudocleavage furrows are present, more defined dots of actin and dAPC2 staining are sometimes observed (Fig. 3, I–P, arrows) in the region of the centrosomes. In one of our wild-type stocks, which was infected with the bacterial endosymbiont *Wolbachia* (visible as small propidium iodide–positive bodies), we saw an additional APC2 localization. *Wolbachia* associate with astral MTs in *Drosophila* and thereby disperse into newly formed cells (Callaini et al., 1994; Kose and Karr, 1995). In infected embryos, dAPC2 localizes with the actin cytoskeleton as in uninfected stocks, and also associates with bacteria at the asters (Fig. 3 D). Another astral MT-associated protein, the kinesin-like protein KLP67A, is also reported to associate with bacteria (Pereira et al., 1997). EM studies have shown that the bacteria are encapsulated within a cytoplasmic vacuole attached to astral MTs via an electron-dense bridge, possibly composed of cellular MT-associated proteins (Callaini et al., 1994). dAPC2's localization to the aster region of noninfected embryos and its association with bacteria suggest that dAPC2 may contribute to the binding of the vacuole to the asters.

After cellularization, dAPC2 is still enriched in the region of MTs. Increased levels of cytoplasmic dAPC2 are observed in mitotic domains (groups of cells undergoing synchronous mitosis) (Fig. 4 D). Here, cytoplasmic condensations of dAPC2 are observed in the region of the spindle in metaphase and anaphase (Fig. 4, E and F, arrows), but are absent in prophase or telophase (the other cells in the mitotic domain in Fig. 4, E and F, are in prophase); serial sections revealed that these cytoplasmic condensations are most prominent within 2–4 μm of the cell apex. In mitotic domains of a *Wolbachia*-infected strain, we observed punctate condensations of dAPC2 near the spindle poles, presumably astrally associated bacteria (Fig. 4 G), consistent with dAPC2 localization to bacteria associated with preblastoderm asters.

dAPC2 is also expressed in dividing cells of the larval brain (Fig. 5). The optic lobes contain two proliferative regions, the inner and outer proliferative zones. dAPC2 is highly expressed in dividing cells of the proliferative zones and in their immediate progeny, but not in differentiated neurons (Fig. 5, A and C). In contrast, Arm is not enriched in the proliferative zones (Fig. 5, B and D) but is enriched in axons. In the ventral nerve cord, Arm is found in axons, whereas dAPC2 is found in midline glial cells (Fig. 5, C and D). In contrast, dAPC localizes to axons, at least in embryos (Hayashi et al., 1997).

However, in larval neuroblasts (neural stem cells) dAPC2 and Arm share a striking asymmetric distribution. Neuroblasts divide asymmetrically to produce a large neuroblast and a smaller ganglion mother cell, which will divide symmetrically to produce two neurons (for review see Fuerstenberg et al., 1998). The asymmetric division requires specific orientation of the mitotic spindle. Inscuteable (Insc), localized in a crescent opposite the future daughter cell during prophase and metaphase, is required for both spindle orientation and localization of the neural determinants Prospero and Numb (Kraut et al., 1996). In larval neuroblasts, both dAPC2 (Fig. 5 E, arrow) and Arm (Fig. 5 F, arrow) colocalize to a cortical crescent next to the future daughter cell; this crescent also includes the neural determinant Prospero (Fig. 5, H and I, arrow). In contrast to other asymmetric neuroblast components (for

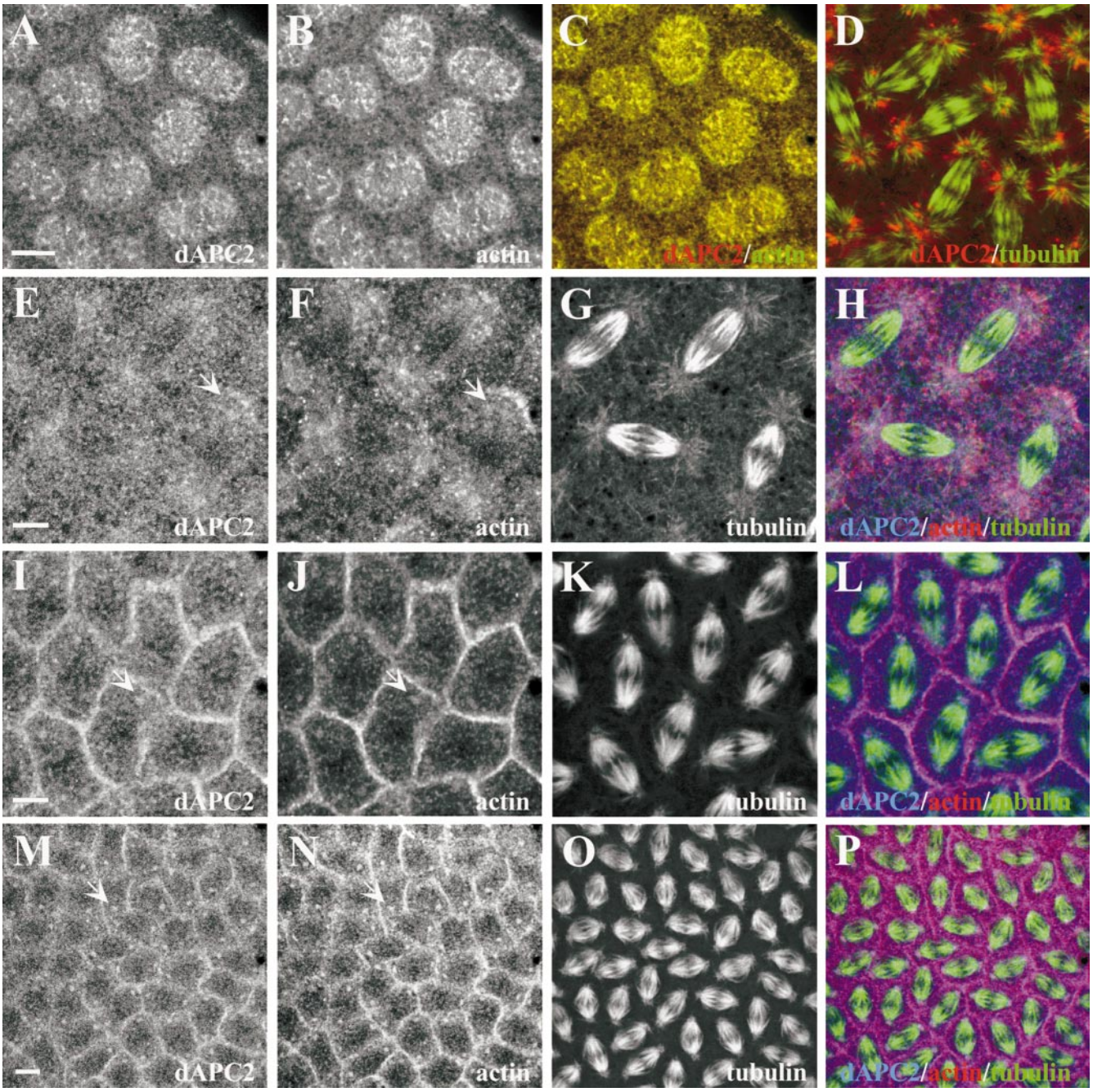

Figure 3. dAPC2 associates with actin in preblastoderm embryos. (A–C and E–P) Wild-type embryos labeled for dAPC2 (A, E, I, and M), actin (B, F, J, and N), and β-tubulin (G, K, and O). In the merged images of the triple-labeled wild-type embryos (H, L, and P), dAPC2 is blue, actin is red, and β-tubulin is green. (A–C) dAPC2 precisely colocalizes with actin in apical bud microvilli. (E–H) During cycle 10, dAPC2 and actin colocalize in halos in the region of the asters (arrows). (I–L) During cycle 11, dAPC2 and actin colocalize in the pseudocleavage furrows and in condensations at the centrosome (arrows). (M–P) During cycle 12, strong condensations of dAPC2 and actin were observed at the centrosome (arrows). (D) dAPC2 (red), β-tubulin (green). In embryos infected by *Wolbachia*, dAPC2 colocalizes with the bacteria at the asters. Bars: (A–H, M–P) 5 μm; (I–L) 7 μm.

review see Fuerstenberg et al., 1998), the dAPC2 and Arm crescents are present even at interphase (Fig. 5 E, lower neuroblast). In some neuroblasts, cortical actin also accumulates in a crescent with dAPC2 (Fig. 5, J and K, arrows), whereas in others this association is less apparent (Fig. 5, L and M, arrows). To examine the relationship between dAPC2 and the spindle, we triple-labeled neuroblasts with antibodies against phosphohistone, β-tubulin, and dAPC2 (Fig. 5, N–P). One pole of the spindle apparatus colocalizes with the dAPC2 crescent; dAPC2 is enriched at this point relative to the rest of the crescent (Fig. 5, O and P, arrows). We also observed low levels of dAPC2 at the opposite cortex at this stage of the cell cycle, the position of which often coincided with the other spin-

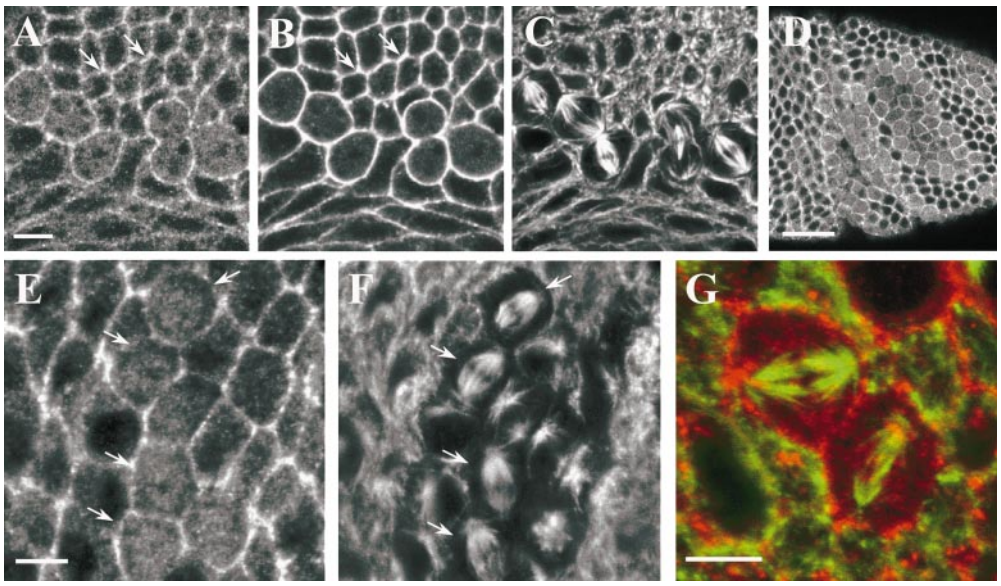

Figure 4. dAPC2 is associated with the cortex in cellularized embryos and with cytoplasmic condensations in dividing cells. (A–C) Wild-type embryos triple-labeled for dAPC2 (A), actin (B), and β-tubulin (C). dAPC2 is associated with the cortex in a punctate distribution corresponding to enrichments of actin (arrows). dAPC2 is not associated with actin at cleavage furrows. (D) Mitotic domain stained for dAPC2. Cytoplasmic dAPC2 is enhanced in dividing cells. (E and F) Wild-type mitotic domain stained for dAPC2 (E) and β-tubulin (F). Cytoplasmic condensations of dAPC2 were observed in the region of the spindle in dividing cells (arrows). (G) Mitotic domain in a *Wolbachia*-infected embryo stained for dAPC2 (red) and β-tubulin (green). dAPC2 is associated with bacteria in the region of the asters. Bars: (A–C, E–G) 5 μm; (D) 20 μm.

dle pole (Fig. 5, O and P, arrows). Whereas cortical dAPC2 associated with spindle poles, neuroblasts did not have cytoplasmic condensations of dAPC2 around the central spindle as were observed in epidermal cells. dAPC2 is also asymmetrically localized in embryonic neuroblasts (Fig. 5 G, arrows).

In nondividing cells, dAPC2 also associates with the cell cortex, and colocalizes with actin. In the embryo, dAPC2 is most strongly expressed in the epidermis and other epithelial cells. In the epidermis, dAPC2 is enriched at the cell cortex and is also found throughout the cytoplasm in a punctate distribution (Fig. 4 A). At the cortex, dAPC2 appears as numerous punctate condensations of protein (Fig. 4 A) which are most prevalent at the apical end of the lateral cell surface but are also found more basally. The most intense staining of dAPC2 appears at points of contact between multiple epidermal cells (Fig. 4 A, arrows). dAPC2 condensations often colocalize with condensations of actin (Fig. 4, A and B, arrows) and phosphotyrosine (data not shown), although actin and phosphotyrosine associate with the cortex more continuously. In fully polarized epithelial cells like the embryonic hindgut (Fig. 6, A and B) or the larval imaginal discs (Fig. 6, C and D), dAPC2 is enriched in adherens junctions, where it colocalizes with Arm; dAPC2 also accumulates on the apical plasma membrane (Fig. 6, A and C). The intracellular distribution of dAPC2 (Fig. 6 E), in contrast to that of Arm (Fig. 6 F), is not modulated in a segmental fashion. A strikingly different localization of dAPC2 occurs in the epidermis after stage 15. dAPC2 becomes organized into very large apical structures in segmentally repeated subsets of ventral epidermal cells (Fig. 6, G and H), just before the stage at which these cells initiate denticle formation. The dAPC2 structures occur specifically in anterior epidermal cells of each segment and colocalize with similar actin structures (Fig. 6, I–K), which likely represent larval denticle precursors.

Although dAPC2 colocalizes with actin in many tissues, it does not colocalize with actin in all contexts. For example, during cellularization, actin is prominent at the cellularization front, whereas dAPC2 is enriched at the apical cortex (data not shown). In addition, as we noted previously, at the cortex of epidermal cells actin is present at the membrane in a continuous fashion, whereas dAPC2 is restricted to regions of most intense actin staining. Finally, dAPC2 is not found with actin in cytokinesis furrows (Fig. 4, A and C). Thus, although dAPC2 associates with the actin cytoskeleton, the context-dependent nature of this association suggests that it is regulated.

Biochemical Properties of dAPC2

Biochemical analyses also suggest that dAPC2 associates with the cell cortex. When we fractionated 0–6-h-old embryos into soluble (S100) and membrane-associated (P100) fractions, dAPC2 partitioned almost equally into these two fractions (Fig. 7 A). In contrast, Arm was almost exclusively in the membrane fraction at this stage. The isoforms of dAPC2 in the membrane fraction migrated more rapidly on SDS-PAGE than those in either the soluble fraction or the total cell lysate (Fig. 7 A); because these isoforms are not detectable in total lysate, we suspect that they may arise during fractionation by dephosphorylation. To examine whether dAPC2 might associate with the membrane via a glycoprotein, we used Con A–Sepharose, which can be used to isolate membrane glycoproteins as well as proteins associated with them (e.g., Arm) (Peifer, 1993). A subset of dAPC2 specifically bound to Con A in extracts from 0–6-h embryos (Fig. 7 A; BicD was a negative control). Thus, dAPC2 may be anchored to the cortex via a transmembrane glycoprotein.

Identification of a dAPC2 Mutation

We mapped *dAPC2* to polytene region 95F1–2 on the

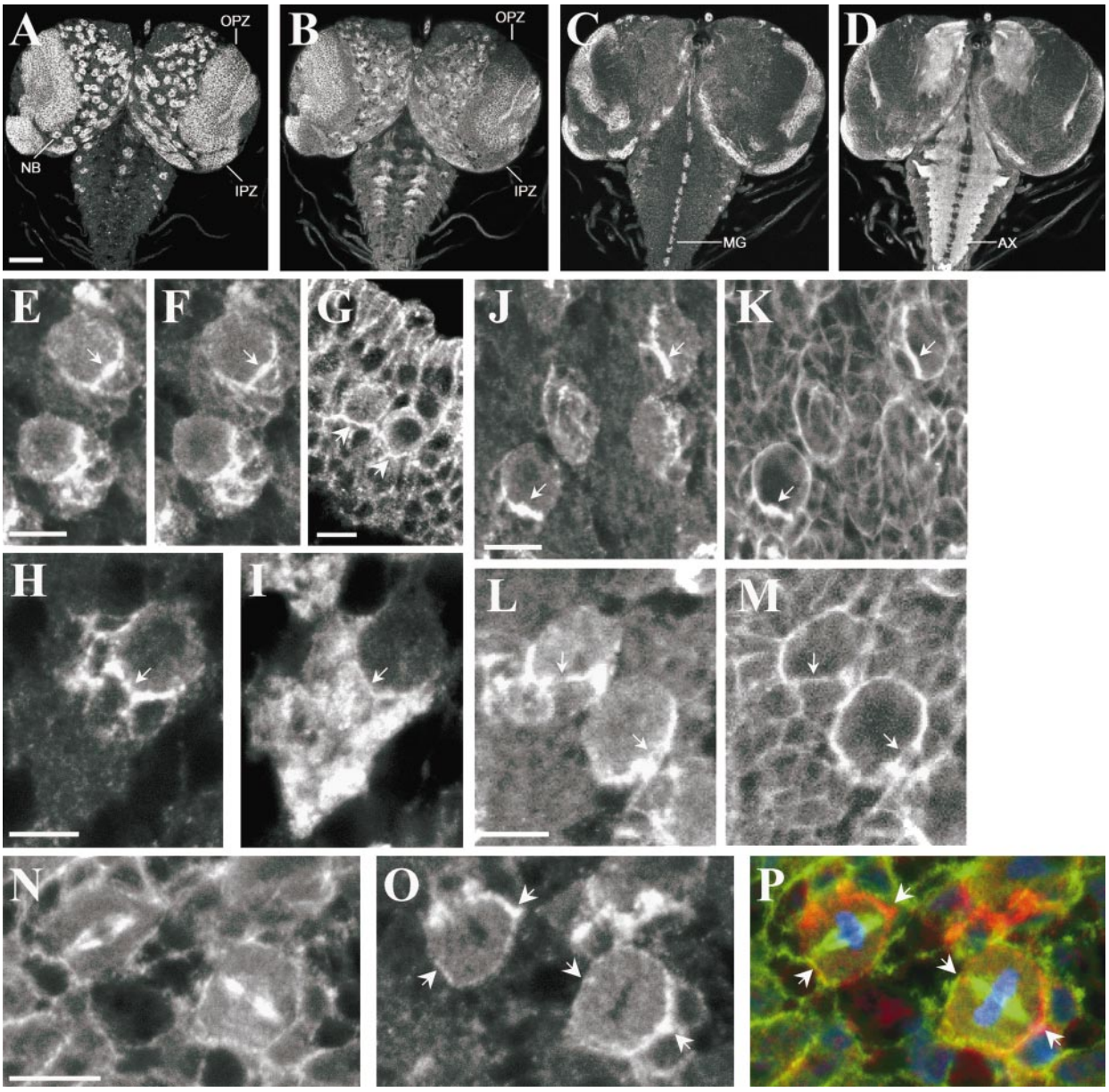

Figure 5. dAPC2 localization in dividing cells of the larval brain. (A–D) Third instar larval brain and ventral nerve cord double-labeled for dAPC2 (A and C) and Arm (B and D). OPZ, outer proliferative zone; IPZ, inner proliferative zone; NB, neuroblasts; MG, midline glia; AX, axons. (E, F, H, I, and J–M) Larval neuroblasts double-labeled for dAPC2 (E, H, J, and L), Arm (F), Prospero (I), and actin (K and M). dAPC2, Arm, and Prospero are asymmetrically localized at the cortex of neuroblasts. Actin is sometimes observed in crescents (K and M). (G) Embryonic neuroblasts labeled for dAPC2 reveal an asymmetric distribution (arrows). (N–P) Larval neuroblasts triple-labeled for β-tubulin (N and P, green), dAPC2 (O and P, red), and phosphohistone (P, blue). Condensations of dAPC2 occur in the region of the spindle poles (arrows). Bars: (A–D) 50 μm; (E–P) 10 μm.

third chromosome by in situ hybridization to wild-type and deficiency chromosomes. *dAPC2* is removed by *Df(3R)crb89-4* and *Df(3R)crb87-4* but not by *Df(3R) crb87-5* (data not shown). All three deficiencies remove *crumbs* and thus have a null *crumbs* phenotype (Tepass and Knust, 1990); thus, the severe epidermal fragmentation made examination of cuticular pattern impossible. During a genetic screen for suppressors of *wg*, we isolated a temperature-sensitive mutation which mapped to this genomic interval by complementation with the same deficiencies, and had a phenotype consistent with that of a negative regulator of Wg signaling (see below). Thus, we evaluated it as a candidate *dAPC2* mutation, sequencing *dAPC2* from the mutant and comparing its sequence to that of *dAPC2* in the parental stock from which the mutant was derived, and in several other wild-type stocks. The mutant and parental chromosomes share 33 polymorphisms relative to the wild-type Canton S; only 8 altered the protein, and most changes are conservative (Fig. 1 D). There is only a single difference between the parental chromosome and the mutant: deletion of three nucleotides, leading to deletion of serine 241. This serine residue

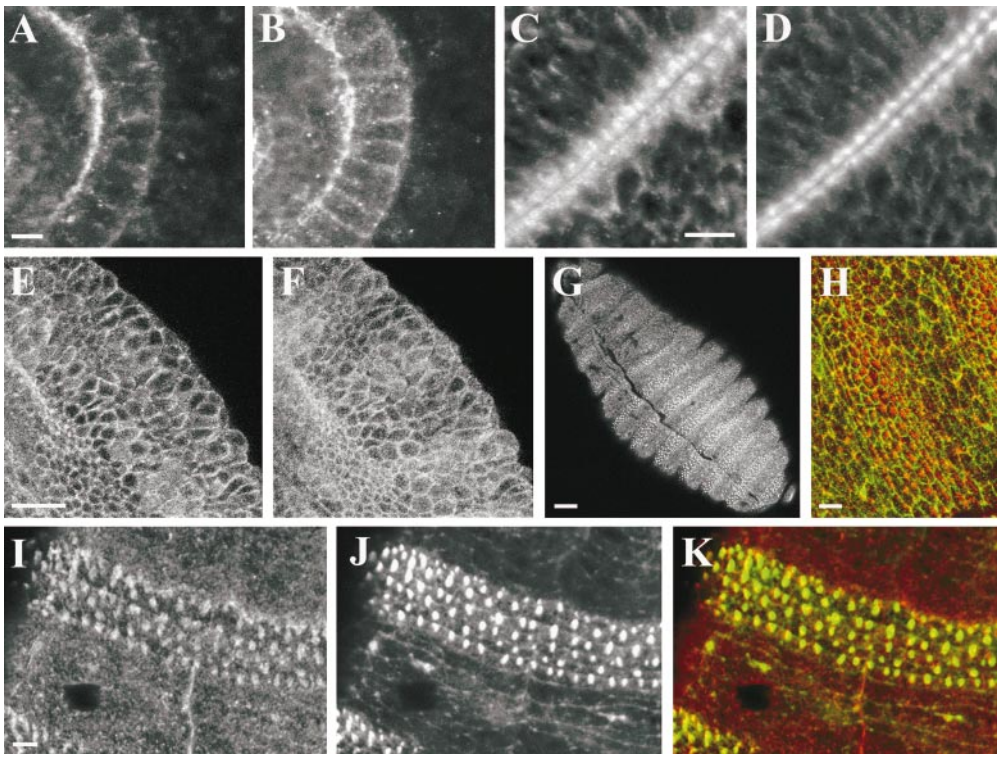

Figure 6. Localization of dAPC2 in epidermal and epithelial cells. The embryonic hindgut (A and B), wing imaginal disc (C and D), and early epidermis (E and F), double-labeled for dAPC2 (A, C, and E) and Arm (B, D, and F). (G) Stage 15 embryo labeled for dAPC2. Stripes of strong dAPC2 accumulation occur in the position of the developing denticles. (H) Stage 15 embryo double-labeled for dAPC2 (red) and Arm (green). Arm does not strongly colocalize with dAPC2 at the denticles. (I–K) Stage 15–16 embryo double-labeled for dAPC2 (I and K, red) and actin (J and K, green). They colocalize in the developing denticle. Bars: (A–D, H–K) 5 μm; (E–G) 25 μm.

falls within an alpha-helix in the third Arm repeat (by analogy to the Arm repeats of β-catenin) (Fig. 1 D). The length of this alpha-helix is invariant among APC family members, and this residue is either serine or alanine (a conservative change) in all APCs. Thus, we refer to this allele as *dAPC2*$^{\Delta S}$.

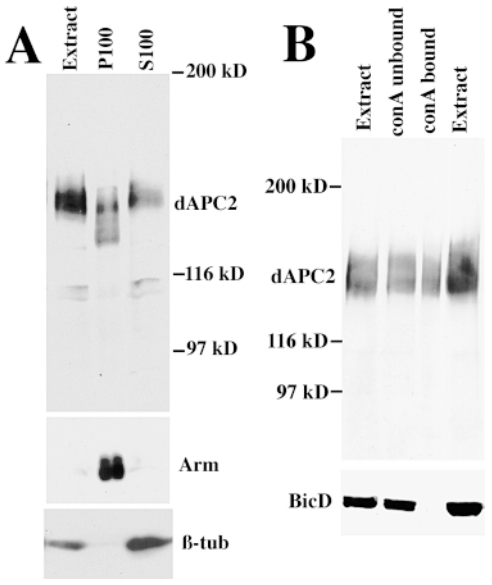

Figure 7. Biochemical properties of dAPC2. (A) dAPC2 is found in the membrane fraction. 0–6-h embryonic extract was fractionated into membrane (P100) and soluble (S100) fractions, and sequentially immunoblotted with anti-dAPC2, anti-Arm, and anti–β-tubulin. Arm and β-tubulin mark the different fractions. (B) A fraction of dAPC2 is bound to Con A. 0–6-h embryonic extract was fractionated using Con A–Sepharose, and sequentially immunoblotted with anti-dAPC2 and anti-BicD (a negative control).

Whereas homozygous mutant embryos accumulate normal levels of dAPC2, mutant dAPC2 migrates more rapidly on SDS-PAGE than wild-type protein (Fig. 8 M). A portion of dAPC2 in heterozygous mutants, which are wild-type in phenotype, also migrates abnormally (data not shown), suggesting that this is an intrinsic property of mutant dAPC2 rather than a consequence of the mutant phenotype. The subcellular localization of dAPC2 in *dAPC2*$^{\Delta S}$ mutants was dramatically altered at both the permissive (18°C) and restrictive (25°C) temperatures. At the restrictive temperature, dAPC2 association with the cell cortex is essentially abolished, rendering the protein almost completely cytoplasmic (Fig. 8 A vs. Fig. 8 D). At the permissive temperature, some cortical dAPC2 remains (Fig. 8 C). In heterozygotes, dAPC2 protein localization is intermediate between mutant and wild-type, as if mutant protein localizes incorrectly despite the presence of wild-type protein (Fig. 8 B). The loss of phosphorylated dAPC2 isoforms observed above (Fig. 8 M) may be a consequence of the loss of cortical association.

We also examined the localization of dAPC$^{\Delta S}$ mutant protein at the restrictive temperature in other tissues. Although dAPC$^{\Delta S}$ is found in apical buds in the preblastoderm embryo (Fig. 8, E and F), it no longer associates with actin structures as does the wild-type protein (Fig. 3, A–C). Furthermore, dAPC2$^{\Delta S}$ (Fig. 8 G) does not associate with the apical plasma membrane in the wing imaginal epithelia, marked by the presence of cortical actin (Fig. 8 H). In the larval neuroblasts, dAPC2$^{\Delta S}$ is largely cytoplasmic (Fig. 8, I and J), although an association with the cortex is sometimes observed (Fig. 8 I, arrow).

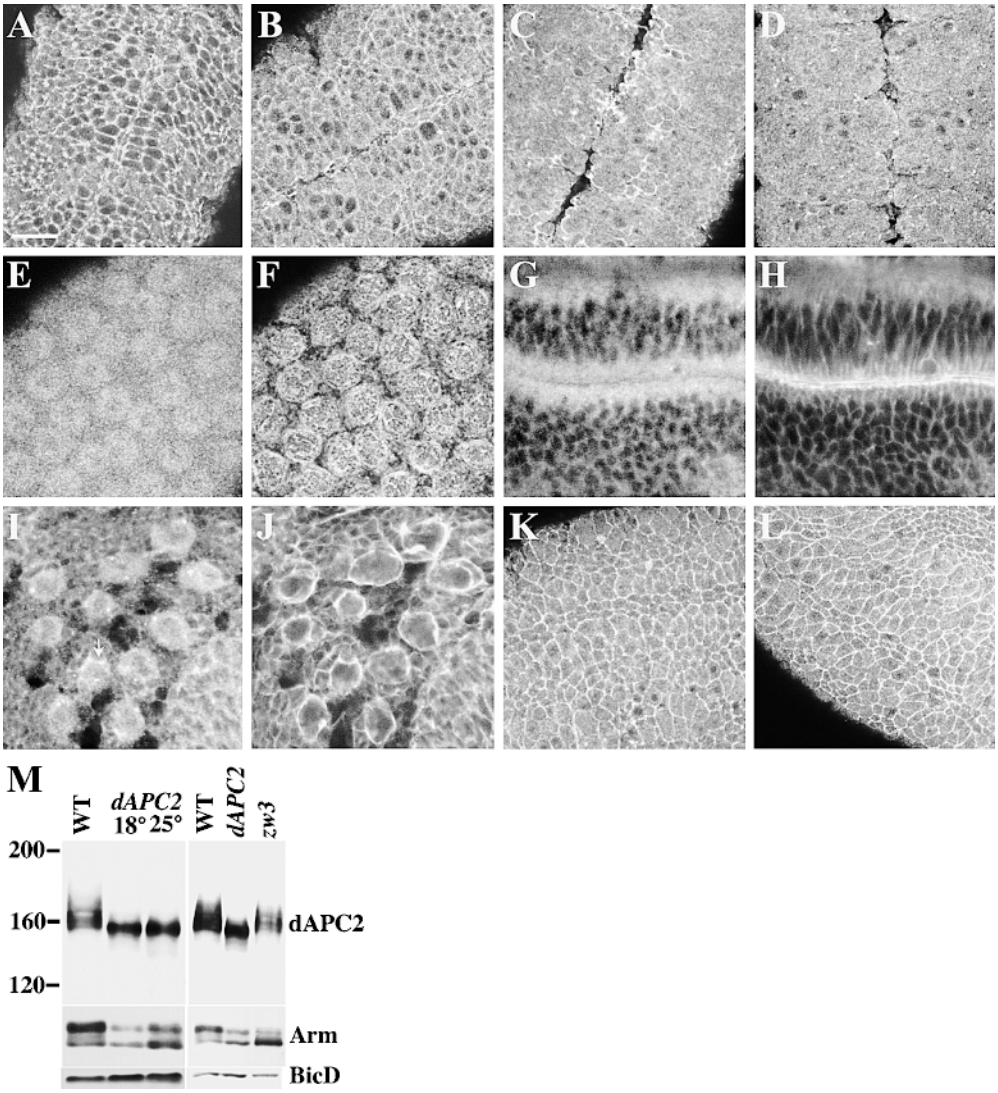

Figure 8. $dAPC2^{\Delta S}$ mutant protein is mislocalized. Embryos in A–D, K, and L are stage 9 of development. (A) Wild-type embryo labeled for dAPC2. dAPC2 is localized to the cell cortex and the cytoplasm. (B) $dAPC2^{\Delta S}$/+ embryo displays less cortical and more cytoplasmic dAPC2. (C and D) In embryos homozygous for $dAPC2^{\Delta S}$ cortical association of dAPC2 is largely abolished. This phenotype is more severe at the restrictive temperature (D, 25°C) than at the permissive temperature (C, 18°C). $dAPC2^{\Delta S}$ is found in apical buds (E) but is not associated with actin (F) in preblastoderm embryos. In the wing imaginal epithelium, $dAPC2^{\Delta S}$ (G) is not found in the adherens junction with actin (H). $dAPC2^{\Delta S}$ is localized to the cytoplasm in larval neuroblasts (I), although some cortical $dAPC2^{\Delta S}$ is observed (I, arrow). The neuroblast membranes are labeled with actin (J). (K–L) The localization of dAPC2 is unchanged in embryos ubiquitously expressing Wg (L) compared with wild-type (K). (M) dAPC2 and Arm proteins accumulate as lower molecular weight isoforms in $dAPC2^{\Delta S}$ homozygotes at both the permissive and restrictive temperatures. In *zw3* mutants, dAPC2 protein isoforms are unchanged, whereas the hypophosphorylated isoform of Arm accumulates. BicD is a loading control. Bars: (A–D, I–L) 20 μm; (E and F) 7 μm; (G and H) 10 μm.

dAPC2 Is a Negative Regulator of Wg Signaling in the Embryonic Epidermis

$dAPC2^{\Delta S}$ is viable and fertile at the permissive temperature (18°C). At the restrictive temperature (25°C), $dAPC2^{\Delta S}$ homozygous mutants derived from heterozygous mothers are viable, indicating that maternal contribution of dAPC2 is sufficient for embryonic development. Heterozygous embryos derived from homozygous mutant mothers are wild-type and survive to adulthood, suggesting that zygotic function is also sufficient. Mutant embryos derived from mutant mothers (referred to below as $dAPC2^{\Delta S}$ maternal/zygotic mutants) have severe abnormalities in their embryonic body plan. On the ventral surface, wild-type embryos show segmentally repeated denticle belts interspersed with naked cuticle (Fig. 9 A). In $dAPC2^{\Delta S}$ maternal/zygotic mutants, denticle belts are replaced with an almost uniform expanse of naked cuticle (Fig. 9 B), as is observed when *wg* is ubiquitously expressed (Fig. 9 D). The dorsal surface also has an array of pattern elements marking specific cell fates (Fig. 9 E); cells receiving Wg signal secrete fine hairs. On the dorsal surface of $dAPC2^{\Delta S}$ maternal/zygotic mutants, many more cells secrete fine hairs (Fig. 9 F), as they do when *wg* is ubiquitously expressed (data not shown). Thus, maternal/zygotic loss of *dAPC2* function activates Wg signal transduction both dorsally and ventrally, suggesting that wild-type dAPC2 helps negatively regulate this pathway.

Perturbing *dAPC2* function at defined developmental time points supports this hypothesis. At the permissive temperature, *dAPC2* mutant embryos develop normally into adults and a homozygous mutant stock can be maintained. When we shifted homozygous mutant embryos up to the restrictive temperature at 4 h after egg laying (AEL), they secreted uniform naked cuticle, like animals at the restrictive temperature throughout development. Progressively later upshifts result in intermediate cuticle defects, with increasing numbers of denticles secreted, until by 10 h AEL the pattern is essentially wild-type (data

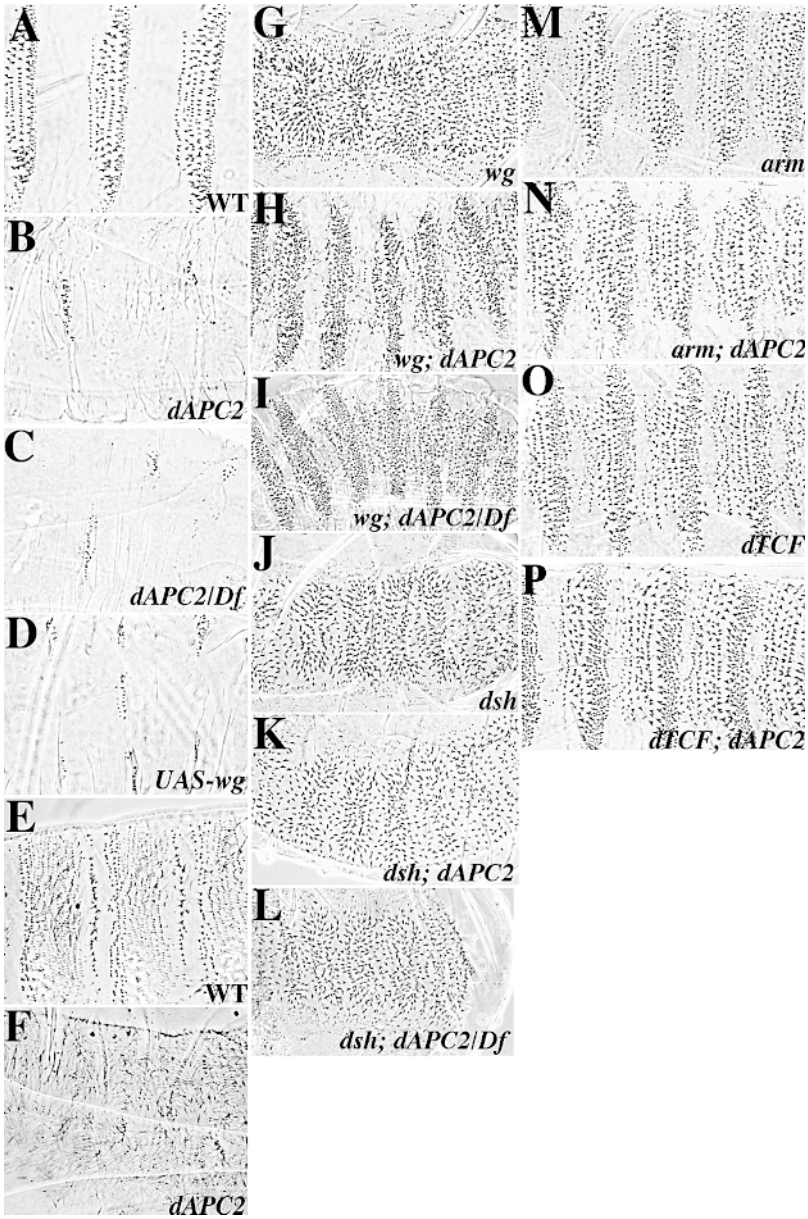

Figure 9. dAPC2 is a negative regulator of Wg signaling. (A) Wild-type cuticle pattern with alternating denticle belts and naked cuticle. (B) $dAPC2^{\Delta S}$ maternal/zygotic mutants show excess naked cuticle. (C) $dAPC2^{\Delta S}/Df(3)crb87\text{-}4$ embryos derived from $dAPC2^{\Delta S}/Df(3)crb87\text{-}4$ mothers are indistinguishable from $dAPC2^{\Delta S}$ homozygotes. (D) Embryo ubiquitously expressing upstream activation sequence (UAS)-Wg via the *e22c-GAL4* driver. (E) Dorsal surface of a wild-type embryo. (F) Dorsal surface of a $dAPC2^{\Delta S}$ maternal/zygotic mutant, covered with a uniform lawn of fine hairs. (G) wg^{CX4} (null) with a lawn of uniform denticles. (H and I) wg^{CX4}; $dAPC2^{\Delta S}$ homozygote (H) and wg^{CX4}; $dAPC2^{\Delta S}/Df(3R)crb87\text{-}4$ mutant (I) derived from $dAPC2^{\Delta S}$ mutant mother. The pattern is substantially but not completely rescued. (J, K, and L) dsh^{75} maternal/zygotic mutants (J), dsh^{75}; $dAPC2^{\Delta S}$ maternal/zygotic double mutants (K), and dsh^{75}; $dAPC2^{\Delta S}$ maternal/dsh^{75}/Y; $dAPC2^{\Delta S}/Df(3R)crb87\text{-}4$ zygotic mutants (L) are indistinguishable, with a *wg*-null–like phenotype. (M and N) $arm^{H8.6}$ homozygotes (M) and $arm^{H8.6}$; $dAPC2^{\Delta S}$ homozygous embryos derived from $dAPC2^{\Delta S}$ mutant mothers (N) are indistinguishable, with a weak *wg*-like phenotype. (O and P) $dTCF^{3}$ homozygotes (O) and $dAPC2^{\Delta S}$; $dTCF^{3}$ homozygous embryos from $dAPC2^{\Delta S}$ mutant mothers (P) are indistinguishable, with a weak *wg*-like phenotype.

not shown). Conversely, shifts from the restrictive temperature down to the permissive temperature at 4 h AEL fully rescue the pattern, whereas progressively later downshifts result in more and more naked cuticle replacing the ventral denticle belts. Thus, *dAPC2* activity is required between 4–10 h AEL, the same time window during which *wg* acts (Bejsovec and Martinez-Arias, 1991; Heemskerk et al., 1991). Somewhat surprisingly, *dAPC2* function may be dispensable for adult patterning; mutant embryos shifted up to the restrictive temperature after 10 h and cultured continuously at this temperature develop into apparently normal adults. This could be the result of partial activity of the $dAPC2^{\Delta S}$ allele. However, we suspect that $dAPC2^{\Delta S}$ is at least a strong hypomorph, as placing this allele over a deficiency for the region both in the mother and the zygote, does not increase the severity of the embryonic mutant phenotype at restrictive temperature (Fig. 9 C).

We carried out epistasis analysis to position *dAPC2* with respect to other components of the signal transduction pathway. *wg;* $dAPC2^{\Delta S}$ double mutant embryos (with $dAPC2^{\Delta S}$ mutant mothers) show a partial rescue of the *wg* phenotype, with restoration of the normal diversity of cuticular pattern elements and small expanses of naked cuticle (Fig. 9, G and H), suggesting that *dAPC2* is downstream of *wg*. There are two possible explanations for the fact that the double mutant does not show the same phenotype as the *dAPC2* single mutant: either $dAPC2^{\Delta S}$ is not null, or the negative regulatory machinery remains partially active in the absence of dAPC2. If $dAPC2^{\Delta S}$ is not null, we reasoned that repeating the epistasis test with $dAPC2^{\Delta S}$ in trans to a deficiency removing *dAPC2 (Df(3R)crb87-4)* might further reduce dAPC2 function, producing a double mutant phenotype more similar to that of $dAPC2^{\Delta S}$ alone. However, when we did this, there was no change in the double mutant phenotype (Fig. 9 I), sug-

gesting that *dAPC2*$^{\Delta S}$ may be genetically null for this function. Other components of the Wg signal transduction pathway act downstream of *dAPC2*. Embryos maternally and zygotically mutant for both *dishevelled* (*dsh*) and *dAPC2* (Fig. 9 K) show a phenotype indistinguishable from the *dsh* single mutant (Fig. 9 J), as do embryos maternally mutant for both *dsh* and *dAPC2* that are zygotically *dsh/Y; dAPC2*$^{\Delta S}$*/Df(3R)crb87-4* (Fig. 9 L). Likewise, *arm; dAPC2* and *dAPC2; dTCF* double mutants (derived from dAPC2 homozygous mothers) (Fig. 9, N and P) are indistinguishable from *arm* or *dTCF* single mutants (Fig. 9, M and O). Thus, *dsh*, *arm*, and *dTCF* all act genetically downstream of *dAPC2*; this was expected for *arm* and *dTCF*, but was surprising for *dsh*.

Loss of *dAPC2* also leads to ectopic activation of Wg-responsive genes. One target is *wg* itself. If the Wg pathway is constitutively activated by removing *zw3* function (Siegfried et al., 1992) or by expressing constitutively active Arm (Pai et al., 1997), an ectopic stripe of *wg* RNA is induced in each segment. A similar ectopic stripe of *wg* RNA is seen in *dAPC2*$^{\Delta S}$ maternal/zygotic mutants (Fig. 10, A and B). Similarly, the domain of expression of a second Wg target gene, *engrailed* (*en*), is expanded relative to wild-type (Fig. 10, G and H), as it is in *zw3* mutants or in the presence of activated Arm. In addition, a novel phenotype was observed. In *dAPC2*$^{\Delta S}$ maternal/zygotic mutants (Fig. 10, D and E), the levels of Wg protein are higher and Wg extends more cell diameters away from *wg*-expressing cells than in wild-type (Fig. 10 C). These effects on Wg protein do not appear to be accounted for solely by ectopic activation of *wg* RNA, as they are detected beginning at stage 9 before induction of ectopic *wg*, and they are not observed in embryos expressing activated Arm (Fig. 10 F). Thus, the efficiency of Wg protein transport (Dierick and Bejsovec, 1998) appears to be enhanced in *dAPC2* mutants.

dAPC2 mutant embryos still respond to Wg signaling, as segmental stripes of stabilized Arm remain (Fig. 10, I and J). In *dAPC2*$^{\Delta S}$ maternal/zygotic mutants, levels of cytoplasmic Arm in all cells are elevated, but cells receiving Wg signal continue to accumulate more Arm than their neighbors (Fig. 10 J). In contrast, *zw3* loss of function results in uniform accumulation of cytoplasmic Arm in all cells, eliminating the Arm stripes (Peifer et al., 1994). Immunoblot analysis of Arm protein from *dAPC2*$^{\Delta S}$ maternal/zygotic mutants revealed an accumulation of hypophosphorylated Arm (Fig. 8 M). This effect was not as dramatic as that seen in a *zw3* mutant (Fig. 8 M), but was similar to that seen upon ubiquitous expression of Wg using the *e22c-GAL4* driver (data not shown). Thus, the effect of *dAPC2*$^{\Delta S}$ on Arm levels is intermediate between that of wild-type and that of *zw3* loss of function, suggesting that negative regulation of Arm is reduced but not completely abolished in *dAPC2*$^{\Delta S}$.

As *dAPC2*$^{\Delta S}$ activates Wg signaling, we examined whether the change in its localization was simply a consequence of pathway activation. When we activated Wg signaling by ubiquitous Wg expression (via the *e22c-GAL4* driver) or by removing *zw3* function, the localization of dAPC2 was essentially unchanged, suggesting that pathway activation is not sufficient to eliminate cortical dAPC2 (Fig.8, K and L; data not shown). There was also

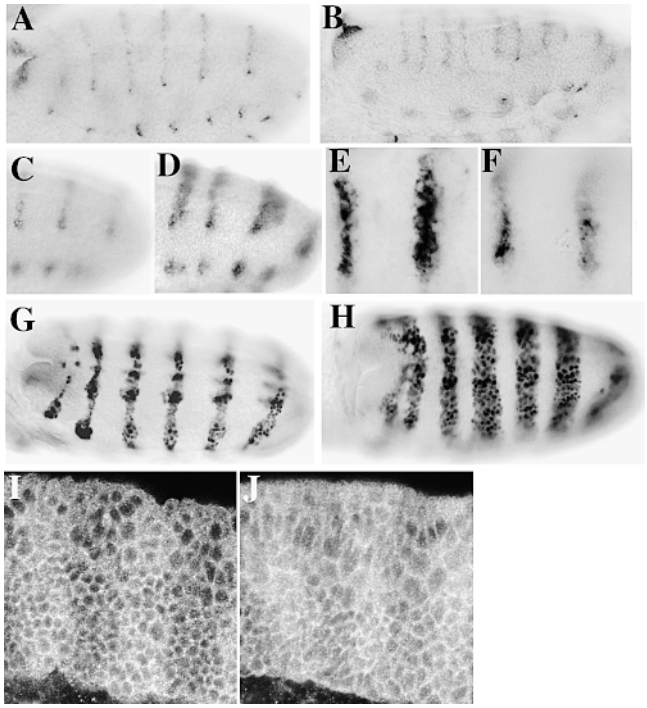

Figure 10. Molecular responses in *dAPC2*$^{\Delta S}$ mutants mimic Wg hyperactivity. (A) Wild-type *wg* RNA is expressed in one row of cells per segment. (B) In *dAPC2*$^{\Delta S}$ maternal/zygotic mutants, an ectopic stripe of *wg* is induced. (C) In wild-type embryos, Wg protein can be detected several cell diameters beyond the mRNA expression domain. (D) Wg is distributed over a greater distance in a *dAPC2*$^{\Delta S}$ maternal/zygotic mutant. (E) Close-up of Wg in *dAPC2*$^{\Delta S}$. (F) Wg in an embryo expressing activated Arm. (G) Wild-type Engrailed expression. (H) Engrailed expression is dramatically expanded in *dAPC2*$^{\Delta S}$ maternal/zygotic mutants. (I) In wild-type embryos, Arm protein is stabilized in cells receiving Wg signal, thus accumulating in broad stripes. (J) In *dAPC2*$^{\Delta S}$ maternal/zygotic mutants, Arm levels rise in both stripe and interstripe cells, but cells receiving Wg still accumulate more Arm.

no apparent change in dAPC2 protein levels or isoforms in *zw3* mutants relative to wild-type (Fig. 8 M); this was somewhat surprising as GSK phosphorylates hAPC (Rubinfeld et al., 1996), and suggests that dAPC2 can be phosphorylated by another kinase.

Discussion

dAPC2 and Wg Signaling

The current model for hAPC function suggests that it is part of the destruction machinery for βcat and thus, negatively regulates Wnt signaling. dAPC negatively regulates the Wg pathway in the *Drosophila* eye (Ahmed et al., 1998), although surprisingly not in other tissues. We examined the function of dAPC2, which shows a broader pattern of expression. dAPC2 interacts directly with Arm and negatively regulates Wg signaling in the embryonic epidermis, helping trigger Arm destruction. *dAPC2* mutant embryos resemble *zw3* mutants in cuticle phenotype and in ectopic activation of Wg target genes. One novel pheno-

type of *dAPC2*$^{\Delta S}$ is a broadening of the stripes of Wg protein, suggesting an effect on Wg transport (Dierick and Bejsovec, 1998). This is not observed when Wg signaling was activated by other means, suggesting that dAPC2 may have novel roles in Wg signaling.

In *zw3* mutants, cytoplasmic Arm levels rise sharply (Peifer et al., 1994). The effect of the *dAPC2*$^{\Delta S}$ mutation on Arm was similar but less severe. The current model for the destruction machinery is that Zw3, Axin, and APC function as a complex, facilitating Arm phosphorylation by Zw3 and thus targeting it for destruction (for review see Polakis, 1999). Axin can bind GSK/Zw3 and βcat/Arm independently of APC. Perhaps in the absence of dAPC2, Zw3 may still phosphorylate Arm, but not as effectively, explaining why loss of dAPC2 affects Arm stability less severely than does loss of Zw3. However, this conclusion is tempered by the fact that *dAPC2*$^{\Delta S}$ is not a protein-null, and in addition, other APC family members may play redundant roles.

Our epistasis tests between *dAPC2* and other components of the Wg pathway generally conform to earlier models of APC function, but also suggest further complexity. As expected, *dAPC2* acts downstream of *wg* and upstream of *arm* and *dTCF*. However, the suppression of *wg* by *dAPC2*$^{\Delta S}$ is incomplete. As above, this may be because *dAPC2*$^{\Delta S}$ is not null, because dAPC2 is not completely essential for Arm downregulation, or because of redundancy. In contrast to *zw3* (Siegfried et al., 1992), *dAPC2*$^{\Delta S}$ is genetically upstream of *dsh*. However, the relative positioning of dAPC2 and Dsh will not be definitive until a protein-null allele of *dAPC2* is available. Most current models place Dsh upstream of the destruction machinery, but the recent discovery that Dsh, along with Axin, APC, and Zw3/GSK, is a component of the destruction complex (Fagotto et al., 1999; Kishida et al., 1999; Smalley et al., 1999) reveals that these proteins may function as a network rather than as a linear series, making the results of epistasis tests more difficult to interpret. For example, the epistasis relationships might be explained if dAPC2 regulated assembly of Dsh into the destruction complex. In the absence of dAPC2, Dsh might constitutively turn off the destruction complex, activating signaling; thus, loss of dAPC2 would have no effect if Dsh is also absent.

The localization of dAPC2 to large membrane-associated structures is intriguing. Axin and Dsh also accumulate in large punctate, often cortical structures when overexpressed in vertebrate cells, and like dAPC2, a fraction of Axin associates with a glycoprotein (Axelrod et al., 1998; Fagotto et al., 1999; Kishida et al., 1999; Smalley et al., 1999). Colocalization experiments will reveal whether cortical dAPC2 puncta contain other components of the destruction machinery. In light of these data, the inability of *dAPC2*$^{\Delta S}$ to associate with the plasma membrane may be informative. Loss of serine 241 likely affects the secondary structure of the Arm repeats, which may affect dAPC2 binding to a protein partner at the membrane. A membrane-bound localization of the destruction complex, perhaps via dAPC2, could be essential for optimal function of the Wg pathway. Both mislocalization of mutant dAPC2$^{\Delta S}$ protein and the slight residual activity of the destruction complex in these mutants could be explained if Arm destruction continues, albeit at greatly reduced levels, in the cytosol. These speculative ideas can be tested in the future by examining colocalization of dAPC2 and other components of the destruction complex in wild-type embryos and in the various mutant backgrounds.

Although dAPC (Ahmed et al., 1998) and dAPC2 clearly negatively regulate the Wg pathway, misexpression of APC in *Xenopus* suggested an apparent positive role in Wnt signaling (Vleminckx et al., 1997). APR-1, the closest *C. elegans* APC relative, also appears to be a positive effector of Wnt signaling (Rocheleau et al., 1997). However, APR-1 is very distantly related to the APC family. APR-1's Arm repeats are only slightly more similar to those of APC than to the Arm repeats of Arm (Fig. 1 B). Whereas APR-1 has two highly divergent SAMP repeats (Rocheleau et al., 1997), it does not contain the conserved NH_2-terminal region or recognizable 15 or 20 amino acid repeats. Perhaps APR-1 is not an APC homologue, but instead plays a distinct role in the pathway.

dAPC2$^{\Delta S}$ adults are viable and morphologically normal, suggesting that dAPC2 may not be required for critical functions such as patterning imaginal discs. Since the phenotypic severity of *dAPC2*$^{\Delta S}$ homozygotes is similar to that of *dAPC2*$^{\Delta S}$*/Deficiency*, this allele is likely to be at least a strong hypomorph for Wg signaling in the embryonic epidermis. Although it is possible dAPC2 only functions there, its widespread expression at other stages suggests otherwise. Whether or not *dAPC2*$^{\Delta S}$ is a null, dAPC2 may still serve other functions. The specific effects of *dAPC2* (these data) and *dAPC* (Ahmed et al., 1998) mutations suggest that in some contexts they may be redundant. The possible other functions of dAPC2 remain to be tested by examining the effect of *dAPC2* mutations on processes such as neuroblast divisions, and by characterizing *dAPC dAPC2* double mutants.

dAPC2 and the Cytoskeleton

Previous studies of APC in vertebrate cultured cells revealed that APC localizes to the membrane and cytoplasm (e.g., Näthke et al., 1996), where it can associate with MTs (Munemitsu et al., 1994; Smith et al., 1994; Näthke et al., 1996). Our biochemical and localization studies of dAPC2 reveal a complex relationship between dAPC2 and the actin and MT cytoskeletons, suggesting potential functions for dAPC2 in regulation of the cytoskeleton.

dAPC2 colocalizes with actin in many but not all cell types, suggesting a regulated interaction. The association between the actin cytoskeleton and dAPC2 may occur via Arm and α-catenin, although in some places where dAPC2 and actin colocalize, there is little or no detectable Arm. The colocalization of dAPC2 and actin is intriguing given the effects of Wnt/Fz signaling on planar polarity in *Drosophila* (for review see Shulman et al., 1998; for possible effects of Wg see Tomlinson et al., 1997). In the wing, the best studied example, Fz signaling triggers asymmetric polymerization of actin, leading to development of an actin-based wing hair in the distal vertex of each hexagonal wing cell (Wong and Adler, 1993). The colocalization of actin and dAPC2 during the onset of denticle formation was particularly striking in this context, because the process of denticle formation is very similar to that of wing hair formation in the nature of the structure, its strict ori-

entation in the plane of the tissue, and in its cell biological and genetic bases. This raises the possibility that Wg/Wnt signaling directly affects the actin cytoskeleton and thus tissue polarity, using dAPC2 as an effector.

Although dAPC2 does not contain the basic region thought to mediate MT association of hAPC, our data are consistent with the possibility that dAPC2, like hAPC (Munemitsu et al., 1994; Smith et al., 1994; Näthke et al., 1996), may associate with MTs under certain circumstances. The data for a microtubule association of dAPC2 are less robust than those suggesting association with actin. Whereas dAPC2 does not prominently localize to most microtubule-based structures (nor does hAPC, unless overexpressed), dAPC2 localized to several places consistent with a role in anchoring microtubules. In preblastoderm embryos, when actin is essential for tethering the spindle to the membrane (for review see Foe et al., 1993), dAPC2 colocalizes with cortical actin and subcortical actin puncta. Subcortical dAPC2 is concentrated just above the spindle, placing it in a position to interact with astral MTs as they reach toward the cortex. Both dAPC2 and actin also localize to a dot-like structure which may be the centrosome. In postblastoderm embryos, dAPC2 is subtly enriched in the vicinity of the spindle.

The asymmetric localization of dAPC2 in dividing neuroblasts is also consistent with a possible role for dAPC2 in linking the spindle to the cortex. During neuroblast mitosis, the spindle is specifically oriented (for review see Fuerstenberg et al., 1998). Insc, which localizes to a crescent opposite the future daughter cell from late interphase through metaphase, coordinates the neuroblast asymmetric cell division (Kraut et al., 1996). Other proteins are likely to act in this process; e.g., Bazooka acts upstream of Insc (Kuchinke et al., 1998). In *C. elegans* (Waddle et al., 1994) and yeast (for review see Heil-Chapdelaine et al., 1999), actin or actin-associated proteins localize asymmetrically in cells in which spindle orientations are specified, suggesting a role for actin in this process. The position of actin in a crescent next to the future daughter cell in a subset of the neuroblasts suggests that actin may affect spindle orientation in *Drosophila* neuroblasts as well. dAPC2 may also play a role in this process. Within the crescent, dAPC2 localization was strongest in the region of the spindle pole. During later stages of mitosis, although dAPC2 remains enriched in a crescent next to the future daughter, dAPC2 also localizes to the cortex on the opposite side of the cell, often in the region of the other spindle pole. In contrast to other asymmetrically localized components of the neuroblast, dAPC2 localizes to a crescent during all stages of the cell cycle; in fact, the dAPC2 crescent was most apparent during interphase and prophase. dAPC2 and actin could also act as polarity markers for other proteins; actin is required for the asymmetric localization of Insc, Prospero, and Staufen (Broadus and Doe, 1997; Knoblich et al., 1997). We emphasize that the dAPC2/MT connection remains speculative. In the future we must directly test whether dAPC2 associates with MTs, whether it can affect spindle orientation, and whether dAPC2 and Arm function in the neuroblast asymmetric cell division.

We raise this issue in light of the influence of Wnt signaling on mitotic spindle orientation in both *C. elegans* embryos (Thorpe et al., 1997) and in *Drosophila* sensory cells (Gho and Schweisguth, 1998). In *C. elegans*, Wnt signaling controls spindle orientation independent of transcription (Schlesinger et al., 1999), suggesting that the Wnt pathway directly targets the cytoskeleton. Since dAPC2 regulates Wg/Wnt signal transduction and appears to have connections to the cytoskeleton, it is a candidate for a direct effector of this process. RNA interference studies of *C. elegans* relatives of Arm (WRM-1) and APC (APR-1) did not reveal defects in spindle orientation (Schlesinger et al., 1999), suggesting the existence of a branch to the cytoskeleton upstream of APC and Arm. However, because RNA interference may not completely remove gene function, and because of the divergence between APR-1 and the APC family noted above, the involvement of Arm and dAPC2 in the pathway remains plausible. These data are also intriguing in light of studies of the hAPC binding protein EB1 (Su et al., 1995), which colocalizes with the spindle, centrosome, and asters (Berrueta et al., 1998; Morrison et al., 1998). Budding and fission yeast EB1 homologues are required for spindle assembly and stability (Beinhauer et al., 1997; Schwartz et al., 1997; Muhua et al., 1998). However, it is worth noting that dAPC2 appears to lack the binding domain for EB1 identified in hAPC.

In summary, our results define a role for *Drosophila* APC2 in the negative regulation of Wg signaling in the embryonic epidermis, and raise the possibility that it may act upstream of Dsh. This supports the idea that different APC family members operate in different tissues. The localization of dAPC2 in vivo, together with previous studies of hAPC in cultured cells, raises the possibility that dAPC2 acts as an effector molecule through which Wnt signaling influences the cytoskeleton. Finally, because dAPC2 associates with the actin cytoskeleton in contexts where no Wg signaling is thought to occur, such as in preblastoderm embryos, dAPC2 may play more fundamental roles in cytoskeletal regulation. Such functions may be revealed by further genetic analyses of *dAPC* and *dAPC2*.

We thank S. Tiong, C. Southern, M. Teachey, and N. Vo for assistance; C. Doe, B. Duronio, T. Karr, P. Polakis, L. Rose, S. Selleck, and B. Theurkauf for tutorials and discussions; and S. Hayashi, E. Wieschaus, U. Tepass, P. Polakis, C. Doe, the Bloomington *Drosophila* Stock Center, the Berkeley *Drosophila* Genome Project, and R. Fehon and the Duke University Comprehensive Cancer Center's Shared Confocal Facility for essential reagents or equipment.

This work was funded by National Institutes of Health grant GM47857, a U.S. Army Breast Cancer Research Program Career Development Award and the Human Frontier Science Program (to M. Peifer), a National Science Foundation Career Award IBN-9734072 and National Science Foundation grant IBN 96-00539 (to A. Bejsovec), a National Research Service Award grant 1 F32 CA79172-01 (to B. McCartney), the National Cancer Institute of Canada (C. Kirkpatrick), and the Nederlandse Kankerbestrijding (A. Baas).

Submitted: 2 June 1999
Revised: 29 July 1999
Accepted: 9 August 1999

Note Added in Proof: While this manuscript was in review, a related work was published by Yu, X., L. Waltzer, and M. Bienz. 1999. *Nature Cell Biol.* 1:144–151.

References

Ahmed, Y., S. Hayashi, A. Levine, and E. Wieschaus. 1998. Regulation of Armadillo by a *Drosophila* APC inhibits neuronal apoptosis during retinal development. *Cell.* 93:1171–1182.

Axelrod, J.D., J.R. Miller, J.M. Shulman, R.T. Moon, and N. Perrimon. 1998. Differential recruitment of Dishevelled provides signaling specificity in the planar cell polarity and Wingless signaling pathways. *Genes Dev.* 12:2610–2622.

Barth, A.I., I.S. Nathke, and W.J. Nelson. 1997. Cadherins, catenins and APC protein: interplay between cytoskeletal complexes and signaling pathways. *Curr. Opin. Cell Biol.* 9:683–690.

Behrens, J., B.-A. Jerchow, M. Würtele, J. Grimm, C. Asbrand, R. Wirtz, M. Kühl, D. Wedlich, and W. Birchmeier. 1998. Functional interaction of an axin homolog, conductin, with β-catenin, APC, and GSK3β. *Science.* 280: 596–599.

Beinhauer, J.D., I.M. Hagan, J.H. Hegemann, and U. Fleig. 1997. Mal3, the fission yeast homologue of the human APC-interacting protein EB-1 is required for microtubule integrity and the maintenance of cell form. *J. Cell Biol.* 139:717–728.

Bejsovec, A., and A. Martinez-Arias. 1991. Roles of *wingless* in patterning the larval epidermis of *Drosophila. Development.* 113:471–485.

Berrueta, L., S.K. Kraeft, J.S. Tirnauer, S.C. Schuyler, L.B. Chen, D.E. Hill, D. Pellman, and B.E. Bierer. 1998. The adenomatous polyposis coli-binding protein EB1 is associated with cytoplasmic and spindle microtubules. *Proc. Natl. Acad. Sci. USA.* 95:10596–10601.

Broadus, J., and C.Q. Doe. 1997. Extrinsic cues, intrinsic cues and microfilaments regulate asymmetric protein localization in *Drosophila* neuroblasts. *Curr. Biol.* 7:827–835.

Callaini, G., G. Riparbelli, and R. Dallai. 1994. The distribution of cytoplasmic bacteria in the early *Drosophila* embryo is mediated by astral microtubules. *J. Cell Sci.* 107:673–682.

Dierick, H.A., and A. Bejsovec. 1998. Functional analysis of Wingless reveals a link between intercellular ligand transport and dorsal-cell-specific signaling. *Development.* 125:4729–4738.

Fagotto, F., E. Jho, L. Zeng, T. Kurth, T. Joos, C. Kaufmann, and F. Costantini. 1999. Domains of axin involved in protein–protein interactions, Wnt pathway inhibition, and intracellular localization. *J. Cell Biol.* 145:741–756.

Foe, V.E., G.M. Odell, and B.A. Edgar. 1993. Mitosis and morphogenesis in the *Drosophila* embryo: point and counterpoint. *In* The Development of *Drosophila.* M. Bate and A. Martinez-Arias, editors. Cold Spring Harbor Laboratory Press, Plainview, NY. 149–300.

Fuerstenberg, S., J. Broadus, and C.Q. Doe. 1998. Asymmetry and cell fate in the *Drosophila* embryonic CNS. *Int. J. Dev. Biol.* 42:379–383.

Gho, M., and F. Schweisguth. 1998. Frizzled signalling controls orientation of asymmetric sense organ precursor cell divisions in *Drosophila. Nature.* 393: 178–181.

Gumbiner, B.M. 1998. Propagation and localization of Wnt signaling. *Curr. Opin. Genet. Dev.* 8:430–435.

Han, M. 1997. Gut reaction to Wnt signaling in worms. *Cell.* 90:581–584.

Hayashi, S., B. Rubinfeld, B. Souza, P. Polakis, E. Wieschaus, and A. Levine. 1997. A *Drosophila* homolog of the tumor suppressor gene adenomatous polyposis coli down-regulates β-catenin but its zygotic expression is not essential for the regulation of Armadillo. *Proc. Nat. Acad. Sci. USA.* 94:242–247.

Heemskerk, J., S. DiNardo, R. Kostriken, and P.H. O'Farrell. 1991. Multiple modes of *engrailed* regulation in the progression towards cell fate determination. *Nature.* 352:404–410.

Heil-Chapdelaine, R.A., N.R. Adames, and J.A. Cooper. 1999. Formin' the connection between microtubules and the cell cortex. *J. Cell Biol.* 144:809–811.

Kishida, S., H. Yamamoto, S.I. Hino, S. Ikeda, M. Kishida, and A. Kikuchi. 1999. DIX domains of dvl and axin are necessary for protein interactions and their ability to regulate beta-catenin stability. *Mol. Cell. Biol.* 19:4414–4422.

Knoblich, J.A., L.Y. Jan, and Y.N. Jan. 1997. The N terminus of the *Drosophila* Numb protein directs membrane association and actin-dependent asymmetric localization. *Proc. Natl. Acad. Sci. USA.* 94:13005–13010.

Kose, H., and T.L. Karr. 1995. Organization of *Wolbachia pipientis* in the *Drosophila* fertilized egg and embryo revealed by an anti-*Wolbachia* monoclonal antibody. *Mech. Dev.* 51:275–288.

Kraut, R., W. Chia, L.Y. Jan, Y.N. Jan, and J.A. Knoblich. 1996. Role of inscuteable in orienting asymmetric cell divisions in *Drosophila. Nature.* 383: 50–55.

Kuchinke, U., F. Grawe, and E. Knust. 1998. Control of spindle orientation in *Drosophila* by the Par-3-related PDZ-domain protein Bazooka. *Curr. Biol.* 8:1357–1365.

Morrison, E.E., B.N. Wardleworth, J.M. Askham, A.F. Markham, and D.M. Meredith. 1998. EB1, a protein which interacts with the APC tumor suppressor, is associated with the microtubule cytoskeleton throughout the cell cycle. *Oncogene.* 17:3471–3477.

Moser, A.R., A.R. Shoemaker, C.S. Connelly, L. Clipson, K.A. Gould, C. Luongo, W. Dove, P.H. Siggers, and R.L. Gardner. 1995. Homozygosity for the Min allele of Apc results in disruption of mouse development prior to gastrulation. *Dev. Dyn.* 203:422–433.

Muhua, L., N.R. Adames, M.D. Murphy, C.R. Shields, and J.A. Cooper. 1998. A cytokinesis checkpoint requiring the yeast homologue of an APC-binding protein. *Nature.* 393:487–491.

Munemitsu, S., B. Souza, O. Müller, I. Albert, B. Rubinfeld, and P. Polakis. 1994. The APC gene product associates with microtubules in vivo and promotes their assembly in vitro. *Cancer Res.* 54:3676–3681.

Nakagawa, H., Y. Murata, K. Koyama, A. Fujiyama, Y. Miyoshi, M. Monden, T. Akiyama, and Y. Nakamura. 1998. Identification of a brain-specific APC homologue, APCL, and its interaction with beta-catenin. *Cancer Res.* 58: 5176–5181.

Näthke, I.S., C.L. Adams, P. Polakis, J.H. Sellin, and W.J. Nelson. 1996. The adenomatous polyposis coli (APC) tumor suppressor protein localizes to plasma membrane sites involved in active cell migration. *J. Cell Biol.* 134: 165–180.

Pai, L.-M., C. Kirkpatrick, J. Blanton, H. Oda, M. Takeichi, and M. Peifer. 1996. *Drosophila* α-catenin and E-cadherin bind to distinct regions of *Drosophila* Armadillo. *J. Biol. Chem.* 271:32411–32420.

Pai, L.-M., S. Orsulic, A. Bejsovec, and M. Peifer. 1997. Negative regulation of Armadillo, a Wingless effector in *Drosophila. Development.* 124:2255–2266.

Peifer, M. 1993. The product of the *Drosophila* segment polarity gene *armadillo* is part of a multi-protein complex resembling the vertebrate adherens junction. *J. Cell Sci.* 105:993–1000.

Peifer, M., D. Sweeton, M. Casey, and E. Wieschaus. 1994. *wingless* signal and Zeste-white 3 kinase trigger opposing changes in the intracellular distribution of Armadillo. *Development.* 120:369–380.

Pereira, A.J., B. Dalby, R.J. Stewart, S.J. Doxsey, and L.S. Goldstein. 1997. Mitochondrial association of a plus end-directed microtubule motor expressed during mitosis in *Drosophila. J. Cell Biol.* 136:1081–1090.

Polakis, P. 1999. The oncogenic activation of β-catenin. *Curr. Opin. Genet. Dev.* 9:15–21.

Rocheleau, C.E., W.D. Downs, R. Lin, C. Wittmann, Y. Bei, Y.-H. Cha, M. Ali, J.R. Priess, and C.C. Mello. 1997. Wnt signaling and an APC-related gene specify endoderm in early *C. elegans* embryos. *Cell.* 90:707–716.

Rubinfeld, B., I. Albert, E. Porfiri, C. Fiol, S. Munemitsu, and P. Polakis. 1996. Binding of GSK-β to the APC/β-catenin complex and regulation of complex assembly. *Science.* 272:1023–1026.

Schlesinger, A., C.A. Shelton, J.N. Maloof, M. Meneghini, and B. Bowerman. 1999. Wnt pathway components orient a mitotic spindle in the early *Caenorhabditis elegans* embryo without requiring gene transcription in the responding cell. *Genes Dev.* 13:2028–2038.

Schwartz, K., K. Richards, and D. Botstein. 1997. BIM1 encodes a microtubule-binding protein in yeast. *Mol. Biol. Cell.* 8:2677–2691.

Shulman, J.M., N. Perrimon, and J.D. Axelrod. 1998. Frizzled signaling and the developmental control of cell polarity. *Trends Genet.* 14:452–458.

Siegfried, E., T.-B. Chou, and N. Perrimon. 1992. *wingless* signaling acts through zeste-white 3, the *Drosophila* homolog of glycogen synthase kinase-3, to regulate *engrailed* and establish cell fate. *Cell.* 71:1167–1179.

Smalley, M.J., E. Sara, H. Paterson, S. Naylor, D. Cook, H. Jayatilake, L.G. Fryer, L. Hutchinson, M.J. Fry, and T.C. Dale. 1999. Interaction of axin and Dvl-2 proteins regulates Dvl-2-stimulated TCF-dependent transcription. *EMBO (Eur. Mol. Biol. Organ.) J.* 18:2823–2835.

Smith, K.J., D.B. Levy, P. Maupin, T.D. Pollard, B. Vogelstein, and K.W. Kinzler. 1994. Wild-type but not mutant APC associates with the microtubule cytoskeleton. *Cancer Res.* 54:3672–3675.

Su, L.K., M. Burrell, D.E. Hill, J. Gyuris, R. Brent, R. Wiltshire, J. Trent, B. Vogelstein, and K.W. Kinzler. 1995. APC binds to the novel protein EB1. *Cancer Res.* 55:2972–2977.

Tepass, U., and E. Knust. 1990. Phenotypic and developmental analysis of mutations at the *crumbs* locus, a gene required for the development of epithelia in *Drosophila melanogaster. Roux's Arch. Dev. Biol.* 199:189–206.

Thorpe, C.J., A. Schlesinger, J.C. Carter, and B. Bowerman. 1997. Wnt signaling polarizes an early *C. elegans* blastomere to distinguish endoderm from mesoderm. *Cell.* 90:695–705.

Tomlinson, A., W.R. Strapps, and J. Heemskerk. 1997. Linking Frizzled and Wnt signaling in *Drosophila* development. *Development.* 124:4515–4521.

Turner, C.M., and P.N. Adler. 1998. Distinct roles for the actin and microtubule cytoskeletons in the morphogenesis of epidermal hairs during wing development in *Drosophila. Mech. Dev.* 70:181–192.

van Es, J.H., C. Kirkpatrick, M. van de Wetering, M. Molenaar, A. Miles, J. Kuipers, O. Destrée, M. Peifer, and H. Clevers. 1999. Identification of APC2, a homologue of the adenomatous polyposis coli tumour suppressor. *Curr. Biol.* 9:105–108.

Vleminckx, K., E. Wong, K. Guger, B. Rubinfeld, P. Polakis, and B.M. Gumbiner. 1997. Adenomatous polyposis tumor suppressor protein has signaling activity in *Xenopus* embryos resulting in the induction of an ectopic dorsoanterior axis. *J. Cell Biol.* 136:411–420.

Waddle, J.A., J.A. Cooper, and R.H. Waterston. 1994. Transient localized accumulation of actin in *Caenorhabditis elegans* blastomeres with oriented asymmetric divisions. *Development.* 120:2317–2328.

Wieschaus, E., and C. Nüsslein-Volhard. 1986. Looking at embryos. *In Drosophila,* A Practical Approach. D.B. Roberts, editor. IRL Press, Oxford, UK. 199–228.

Wong, L.L., and P.N. Adler. 1993. Tissue polarity genes of *Drosophila* regulate the subcellular location for prehair initiation in pupal wing cells. *J. Cell Biol.* 123:209–221.